

ORIGINAL RESEARCH

Statistical and Functional Studies Identify Epistasis of Cardiovascular Risk Genomic Variants From Genome-Wide Association Studies

Yabo Li ^{ID}, MS;* Hyosuk Cho ^{ID}, BS;* Fan Wang ^{ID}, PhD; Oriol Canela-Xandri ^{ID}, PhD; Chunyan Luo, PhD; Konrad Rawlik ^{ID}, PhD; Stephen Archacki ^{ID}, MD, PhD; Chengqi Xu ^{ID}, PhD; Albert Tenesa ^{ID}, PhD; Qiyun Chen ^{ID}, PhD; Qing Kenneth Wang ^{ID}, PhD, MBA

BACKGROUND: Epistasis describes how gene-gene interactions affect phenotypes, and could have a profound impact on human diseases such as coronary artery disease (CAD). The goal of this study was to identify gene-gene interactions in CAD using an easily generalizable multi-stage approach.

METHODS AND RESULTS: Our forward genetic approach consists of multiple steps that combine statistical and functional approaches, and analyze information from global gene expression profiling, functional interactions, and genetic interactions to robustly identify gene-gene interactions. Global gene expression profiling shows that knockdown of *ANRIL* (DQ485454) at 9p21.3 GWAS (genome-wide association studies) CAD locus upregulates *TMEM100* and *TMEM106B*. Functional studies indicate that the increased monocyte adhesion to endothelial cells and transendothelial migration of monocytes, 2 critical processes in the initiation of CAD, by *ANRIL* knockdown are reversed by knockdown of *TMEM106B*, but not of *TMEM100*. Furthermore, the decreased monocyte adhesion to endothelial cells and transendothelial migration of monocytes induced by *ANRIL* overexpression was reversed by overexpressing *TMEM106B*. *TMEM106B* expression was upregulated by >2-fold in CAD coronary arteries. A significant association was found between variants in *TMEM106B* (but not in *TMEM100*) and CAD ($P=1.9 \times 10^{-8}$). Significant gene-gene interaction was detected between *ANRIL* variant rs2383207 and *TMEM106B* variant rs3807865 ($P=0.009$). A similar approach also identifies significant interaction between rs6903956 in *ADTRP* and rs17465637 in *MIA3* ($P=0.005$).

CONCLUSIONS: We demonstrate 2 pairs of epistatic interactions between GWAS loci for CAD and offer important insights into the genetic architecture and molecular mechanisms for the pathogenesis of CAD. Our strategy has broad applicability to the identification of epistasis in other human diseases.

Key Words: coronary artery disease ■ gene-gene interactions ■ Genome-wide Association Studies ■ long non-coding RNA (lncRNA) *ANRIL* (CDKN2B-AS1) ■ *TMEM106B*

Coronary artery disease (CAD) is the leading cause of death and disability worldwide.^{1,2} CAD is caused by atherosclerosis in coronary arteries, which is initiated by monocyte adhesion to endothelial cells (ECs)

upon stimulation of oxidized low-density lipoprotein and other inflammatory factors.^{1,2} The monocytes then transmigrate across the endothelium into the intima, and differentiate into macrophages, which are

Correspondence to: Qing Kenneth Wang, PhD, MBA, Department of Cardiovascular and Metabolic Sciences, Lerner Research Institute, Cleveland Clinic, 9500 Euclid Avenue/NB5-85, Cleveland, OH 44195. E-mail: wangq2@ccf.org and Qiyun Chen, PhD, Department of Cardiovascular and Metabolic Sciences, Lerner Research Institute, Cleveland Clinic, 9500 Euclid Avenue/NB5-30, Cleveland, OH 44195. E-mail: chengq3@ccf.org

*Li and Cho contributed equally to this work.

For Sources of Funding and Disclosures, see page 20.

© 2020 The Authors. Published on behalf of the American Heart Association, Inc., by Wiley. This is an open access article under the terms of the Creative Commons Attribution-NonCommercial License, which permits use, distribution and reproduction in any medium, provided the original work is properly cited and is not used for commercial purposes.

JAHA is available at: www.ahajournals.org/journal/jaha

CLINICAL PERSPECTIVE

What Is New?

- Coronary artery disease loci identified by GWAS (genome-wide association studies) interact with each other to confer an epistatic effect on risk of the disease, and *ANRIL* locus on chromosome 9p21.3 interacts with the *TMEM106B* locus on 7p21.3, whereas the *MIA3* locus on 1q41 interacts with the *ADTRP* locus on 6p24.1.
- *TMEM106B* expression is upregulated in coronary artery tissue samples from CAD patients, and correlated with downregulation of *ANRIL* (DQ485454); *TMEM106B* modulates the effects of *ANRIL* on endothelial functions involved in atherosclerosis and CAD.
- *ANRIL* is the causal gene for CAD at the 9p21.3 locus, and *TMEM106B* is the causal gene at the 7q21.11 CAD locus.

What Are the Clinical Implications?

- Identification of epistasis is paramount to our understanding of the genetic architecture of a human disease, and may have an important implication on future precision diagnosis and risk stratification of common human diseases based on polygenic risk scores and other methods.
- The causal genes for CAD *ANRIL* and *TMEM106B* may serve as targets for development of drugs and other therapeutic agents to prevent and treat CAD.

Nonstandard Abbreviations and Acronyms

ADTRP	Androgen Dependent TFPI Regulating Protein
ANRIL	Antisense Non-coding RNA in the INK4 Locus
CAD	Coronary Artery Disease
EC	Endothelial Cell
GWAS	Genome-wide Association Studies
HCAEC	Human Coronary Artery Endothelial Cells
MAF	Minor Allele Frequency
MI	Myocardial Infarction
MIA3	MIA SH3 domain ER export factor 3
TMEM100	Transmembrane protein 100
TMEM106B	Transmembrane protein 106B

transformed into foam cells (plaques), the hallmark of atherosclerosis, in the walls of the coronary arteries.^{1,2} The fissure, erosion, and rupture of plaques lead to

possible thrombosis, myocardial infarction (MI) and sudden death.^{1,2} GWAS (genome-wide association studies) have identified >150 genomic loci associated with CAD and MI.³ However, identification of the causal gene(s) under each locus and functional characterization of causal genes are challenging. The first CAD locus on chromosome 9p21.3 identified by GWAS remains the most robust locus.³ More than 50 CAD-associated genomic variants are located at the 9p21.3 CAD locus and multiple candidate genes for CAD were found at the locus, including *ANRIL*, *CDKN2A*, *CDKN2B*, and *MTAP*.⁴ Recently, we showed that the major transcript DQ485454 of *ANRIL*, which encodes a long non-coding RNA, showed significant downregulation in CAD coronary arteries compared with non-CAD arteries.⁵ A series of knockdown and overexpression studies in 2 different endothelial cells (ECs), EA.hy926 cells and human coronary artery endothelial cells (HCAECs), revealed that *ANRIL* regulates EC functions directly involved in atherosclerosis, and suggested that *ANRIL* is involved in the pathogenesis of CAD.⁵

The mechanisms by which *ANRIL* deregulation mediates the development of atherosclerosis are not well understood. We performed global gene expression profiling for *ANRIL*, and showed that knockdown of *ANRIL* downregulated expression of *AHNAK2*, *CLIP1*, *CXCL11*, *ENC1*, *EZR*, *LYVE1*, *WASL*, and *TNFSF10* genes and upregulated *TMEM100* and *TMEM106B* genes.⁵ We functionally characterized the downregulated genes by *ANRIL* knockdown and found that *CLIP1*, *EZR*, and *LYVE1* were involved in modulating the function of *ANRIL* in ECs.⁵ however, the 2 upregulated genes were not functionally characterized further. In this study, we continued these studies, and focused on *TMEM100* on chromosome 17q22 and *TMEM106B* on 7p21.3. *TMEM100* encodes a transmembrane protein 100 with 134 amino acids and 2 hypothetical transmembrane domains. *TMEM100* was shown to be involved in arterial endothelium differentiation and vascular morphogenesis,⁶ endothelial-mesenchymal transformation during atrioventricular canal cushion formation by endocardial calcium signaling,⁷ the maintenance of vascular integrity, and the formation of blood vessels.⁸ *TMEM106B* encodes another transmembrane protein 106 with 274 amino acids and a single pass, type-II transmembrane domain. *TMEM106B* was found to be localized in cellular lysosomes, and regulates lysosome synthesis, size, trafficking, and localization in neurons and cancer cells.^{9–11} The function of *TMEM106B* in cardiovascular cells is unknown.

In this study, we found significant upregulation of the expression level of *TMEM106B*, but not *TMEM100*, in CAD coronary artery tissues and performed mechanistic studies to characterize the function of *TMEM106B* and *TMEM100* in the context of

ANRIL in endothelial cells, including monocyte adhesion to ECs and transendothelial migration of monocytes involved in atherosclerosis. We found that *ANRIL* affects EC functions by regulating the expression of *TMEM106B*, but not *TMEM100*. Genetic analysis revealed that genomic variants in *TMEM106B*, but not in *TMEM100*, were significantly associated with risk of CAD and a significant interaction between the *ANRIL* locus and the *TMEM106B* locus was found in conferring susceptibility of CAD in the UK Biobank. A similar approach also identified a significant interaction between 2 other GWAS loci for CAD, the *ADTRP* locus^{12,13} on chromosome 6p24.1 and the *MIA3* locus^{14,15} on 1q41, also identified for CAD by GWAS.

METHODS

The authors declare that all supporting data are available within the article.

Cell Culture and Transfection

Cell culture and transfection were performed as described by us previously.^{5,16,17} Primary human coronary artery endothelial cells (HCAECs) were cultured in a phenol-red-free endothelial growth medium supplemented with 2% fetal bovine serum (ThermoFisher Scientific, USA), 0.4% human fibroblast growth factor, 0.1% human epidermal growth factor, 0.1% vascular endothelial growth factor, 0.1% insulin-like growth factor, 0.1% ascorbic acid, 0.1% heparin, 0.1% gentamicin/amphotericin-B and 0.04% hydrocortisone. The EAhy926 endothelial cells and HepG2 cells were maintained in DMEM supplemented with 10% fetal bovine serum (ThermoFisher Scientific, USA). Human THP-1 cells were maintained in the RPMI-1640 medium supplemented with 10% fetal bovine serum (ThermoFisher Scientific, USA). All cells were purchased from ATCC (American Type Culture Collection, USA) and cultured at 37°C in a humidified incubator with 5% CO₂. Transfection of mammalian expression plasmid DNA and small interfering RNAs (siRNAs) into HCAECs and EAhy926 cells were performed using the TransIT-X2 Dynamic Delivery System (Mirus Bio, Madison, WI). Transfection of HepG2 cells was performed using Lipofectamine 2000 for plasmid DNA (1 µg), and Lipofectamine RNAi MAX for siRNA (80 nmol/L) according to the manufacturer's protocol (ThermoFisher Scientific).

Human Tissue Samples

This study involved 6 CAD patients and 6 age-matched non-CAD human tissue samples reportedly by Arckacki et al.¹⁸ The mean age was 51±4 years for both CAD

Table. Coronary Artery Tissue Samples

Sample	Age, y	Race and Sex	LAD Blockage	Past Medical History
CAD 1	48	White, M	40%	Cirrhosis
CAD 2	53	White, M	50%	N/A
CAD 3	53	White, M	90%	Stroke
CAD 4	47	White, M	>95%	Drug overdose
CAD 5	50	White, M	100%	Ischemic myopathy
CAD 6	55	White, M	100%	Stroke
Control 1	48	White, M	0%	N/A
Control 2	53	White, M	0%	N/A
Control 3	53	White, M	0%	N/A
Control 4	47	White, M	0%	N/A
Control 5	50	White, M	0%	N/A
Control 6	55	White, M	0%	N/A

Note that each coronary artery disease sample is matched by a non-coronary artery disease control sample (eg, coronary artery disease 1 vs Control 1; coronary artery disease 2 vs Control 2; etc). CAD indicates coronary artery disease.

and control groups (Table). RNA isolation, cDNA synthesis, and reverse transcription-polymerase chain reaction (RT-PCR) analysis was performed as described by us previously.^{5,18–21} We obtained coronary arteries from explanted hearts through the Cleveland Clinic Heart Transplant Program and unmatched or rejected donor hearts from Lifebank of Northeast Ohio as reported.¹⁸ This study was approved by the Cleveland Clinic Institutional Review Board on Human Subject Research and written consent was obtained from the subjects. This study abides by the Declaration of Helsinki principles (Version 2008).

Plasmids and siRNA

A mammalian expression plasmid for *ANRIL* transcript *DQ485454*, referred to as pcDNA3.1-*ANRIL* (DQ485454), was generated by us as described previously.⁵ An expression plasmid for *TMEM106B* was created by subcloning the Mammalian Gene Collection Fully Sequenced Human cDNA clone of *TMEM106B* (GE Dharmacon, USA) into the pcDNA3.1 vector. All plasmids were individually verified by Sanger sequence analysis.

Small interfering RNAs (siRNAs) for *ANRIL*, *TMEM100*, and *TMEM106B* were purchased from IDT (Integrated DNA Technologies) and the negative control siRNA (siNC) was from GE Dharmacon. The sequences of siRNAs are as follows:

ANRIL siRNA: ATCTGTGTTTTTGTCCAATGTCCTT
TMEM100 siRNA: GCUUAGAAGCACUGUUGUAAA
 AATG
TMEM106B siRNA: CUUAUGAUGGAGUCACAUCUG
 AAAA

MIA3 siRNA: GGUGAAGUCUGAAUGCCAUTT
 siNC: Lincode control siRNA (GE Dharmacon, USA)

Real-Time RT-PCR Analysis

Quantitative RT-PCR analysis was performed as described previously by us.^{5,12,22,23} Each sample was run in triplicate and each experiment was repeated at least 3 times. The primer sequences of qRT-PCR are as follows (from 5' to 3'):

ANRIL Forward: CCACATCCCTTGGAGTAATGA
ANRIL Reverse: CCTTTTATCACCCAGCTTCG
GAPDH Forward: GTCTCCTCTGACTTCAACAGCG
GAPDH Reverse: ACCACCCTGTTGCTGTAGCCAA
TMEM100 Forward: ACAGTCCCTCTGGTCAGTGAGA
TMEM100 Reverse: GGCGATGAAGACAACCACAGCA
TMEM106B Forward: CCTACTTGTCTAGGGAACAGG
 AAG
TMEM106B Reverse: AACACAGCCAATCCAGAAAG
 GAG
ADTRP Forward: GCCGCATCCTATGGCTCTACTTTG
ADTRP Reverse: CAAGTAGGTAGATGCTGGCGATGA
MIA3 Forward: TACAAGCGGAGAATTGAAGAAATGG
MIA3 Reverse: GCCAGTTTTTCATGAGCTTTCTTCT

Endothelial Cell Functional Assays

HCAECs or EA.hy926 cells were transfected with plasmids or siRNAs as described above and used for various assays for assessment of endothelial cell functions, including monocyte adhesion to endothelial cells, and transendothelial migration of monocytes, as described by us previously.^{5,19,24–27}

Statistical Analysis

In GWAS, to determine the genetic effects of *TMEM100* and *TMEM106B* on the risk of CAD, 1568 single nucleotide polymorphisms within 100 kb regions spanning the 2 genes were selected from 2 large GWAS data sets for CAD, including CADRDloGRAMplusC4D²⁸ (60 801 cases versus 123 504 controls) and GeneATLAS²⁹ (Key=clinical_c_Block_I20-I25; 33 387 cases versus 418 877 controls). The summary statistics of 1250 single nucleotide polymorphisms was downloaded from their web portals. Each single nucleotide polymorphism was examined for its association with CAD with a meta-analysis of CADRDloGRAMplusC4D and GeneATLAS using statistical program GWAMA³⁰ under the fixed model. To facilitate the meta-analysis, standard error was re-estimated from the reported odds ratio and converted z value. Heterogeneity between the 2 studies was further evaluated for each variant by Cohen's Q tests. If significant heterogeneity (Q<0.05 and I²>70%) was identified, results from the random effect model were reported.

Gene-gene interaction tests between the genetic variant pairs rs2383207 and rs3807865, and rs6903956 and rs17465637 on I20-I25 Ischemic heart diseases (as defined previously,²⁹ clinical_c_Block_I20-I25) was performed using 343 145 unrelated White-British ancestry individuals from UK Biobank. These individuals were a subset of UK Biobank 488 377 genotyped participants, excluding those who failed UK Biobank's own Quality Control because of genotyping missingness rate or heterogeneity, whose sex inferred from the genotypes did not match their self-reported sex and who were not of white British ancestry. We restricted Quality Control even more and removed individuals with a genotype missingness rate >5% across variants. We only kept unrelated individuals, defined as having a Kinship coefficient smaller than 0.0442 between them. A genotypic interaction between the 2 genetic variants along with the main effects of the 2 variants was tested using a Logistic Regression Model where sex, array batch, UK Biobank Assessment Center, age, age², the leading 20 genomic principal components as computed by UK Biobank were added as covariates.

In particular, we used the model:

$$\log\left(\frac{p_i}{1-p_i}\right) = \mu + \mathbf{x}_i^c \beta_c + \mathbf{x}_i^{s1} \beta_{s1} + \mathbf{x}_i^{s2} \beta_{s2} + \mathbf{x}_i^{s1s2} \beta_{s1s2},$$

where p_i is the probability of the individual i being a case. μ is the model mean, \mathbf{x}_i^c is the vector of covariates for individual i , and β_c the vector of covariate effects. \mathbf{x}_i^{s1} and \mathbf{x}_i^{s2} are matrices of dummy binary variables indicating the individual i genotype for the genetic variants $s1$ and $s2$, and β_{s1} and β_{s2} their effects, respectively. The imputed genotypes were called to the genotype with larger probability. Finally, \mathbf{x}_i^{s1s2} is a dummy matrix of binary variables indicating the genotype combination between the genetic variants $s1$ and $s2$ for individual i . β_{s1s2} is the vector of effects. The model was fitted by using the Python StatsModels package. It computes the P value for a particular genotype combination by using a z-test (a z-score is computed as the ratio between the estimated effect and the error, and then the P value is computed by using a normal distribution to perform a 2-tailed test). To preclude possible problems with data sparsity we confirmed that all variants had an MAF (Minor Allele Frequency) >0.28 on the UK Biobank population of European ancestry. The genotype combination having less individuals contained at least 878 individuals for cases and 13 040 for controls for the pair rs2383207 and rs3807865; and 302 individuals for cases and 3731 for controls for the variant pair rs6903956 and rs17465637 for I20-I25 ischemic heart diseases.

Other quantitative data were presented as mean±SD. Statistical analysis was performed with unpaired, 2-tailed Student t tests using the GraphPad

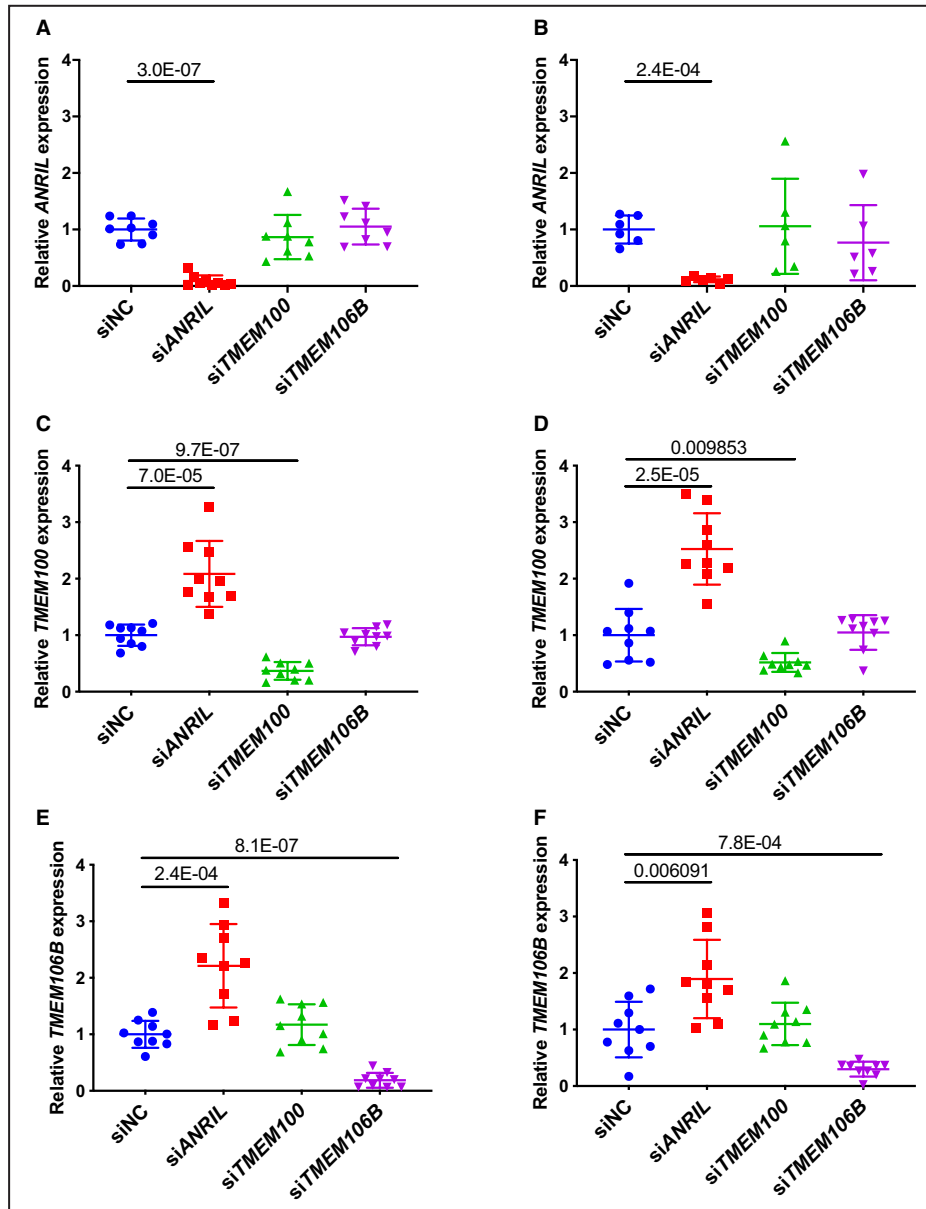


Figure 1. Real-time quantitative reverse transcription-polymerase chain reaction analysis of expression of *ANRIL*, *TMEM100*, and *TMEM106B* in endothelial cells (ECs) transfected with different small interfering (si)RNA.

A, Relative expression of *ANRIL* in EA.hy926 cells transiently transfected with siNC, siANRIL, siTMEM100, or siTMEM106B (n=8 samples/group; 3 wells/experiment with each experiment repeated twice again; data points of ≥ 3 SD were removed as outliers). **B**, Relative expression of *ANRIL* in human coronary artery endothelial cells transiently transfected with siNC, siANRIL, siTMEM100, or siTMEM106B (n=6 samples/group; 3 wells/experiment with each experiment repeated again). **C**, Relative expression of *TMEM100* in EA.hy926 cells transiently transfected with siNC, siANRIL, siTMEM100, or siTMEM106B (n=9 samples/group; 3 wells/experiment with each experiment repeated twice again). **D**, Relative expression of *TMEM100* in human coronary artery endothelial cells transiently transfected with siNC, siANRIL, siTMEM100, or siTMEM106B (n=9 samples/group; 3 wells/experiment with each experiment repeated twice again). **E**, Relative expression of *TMEM106B* in EA.hy926 cells transiently transfected with siNC, siANRIL, siTMEM100, or siTMEM106B (n=9 samples/group; 3 wells/experiment with each experiment repeated twice again). **F**, Relative expression of *TMEM106B* in human coronary artery endothelial cells transiently transfected with siNC, siANRIL, siTMEM100, or siTMEM106B (n=9 samples/group; 3 wells/experiment with each experiment repeated twice again). Statistical analysis was performed using unpaired, 2-tailed Student t tests. Si indicates small interfering.

Prism 8.2.1 software program or the R package. Statistical significance was considered at a P value of ≤ 0.05 . The sample size (n) is indicated for each experiment in figure legends. For qRT-PCR analysis, data of ≥ 3 SD were removed as outliers.

RESULTS

Knockdown of *TMEM106B* Rescues *ANRIL* Knockdown Phenotype of Endothelial Cells Involved in Atherosclerosis

We found that *ANRIL* affects EC functions by regulating the expression of *TMEM106B*, but not *TMEM100*. We first assessed whether knockdown of *TMEM100*

and *TMEM106B* expression using siRNA reverses the effects of knockdown of *ANRIL* expression in 2 types of ECs, EA.hy926 cells (an EC line) and human coronary artery endothelial cells (HCAECs). As shown in Figure 1A through 1F, siRNA for *TMEM100* significantly decreased the expression of *TMEM100*, but not that of *TMEM106B* or *ANRIL* in EA.hy926 cells HCAECs. Similarly, siRNA for *TMEM106B* significantly decreased the expression of *TMEM106B*, but not that of *TMEM100* or *ANRIL*. As previously reported,⁵ *ANRIL* siRNA significantly decreased the expression of *ANRIL* (DQ485454), and increased the expression of *TMEM100* and *TMEM106B* in EA.hy926 and HCAECs (Figure 1A through 1F). In assays for monocyte adhesion to ECs, knockdown of *TMEM100*, but not *TMEM106B*, showed a small but significantly

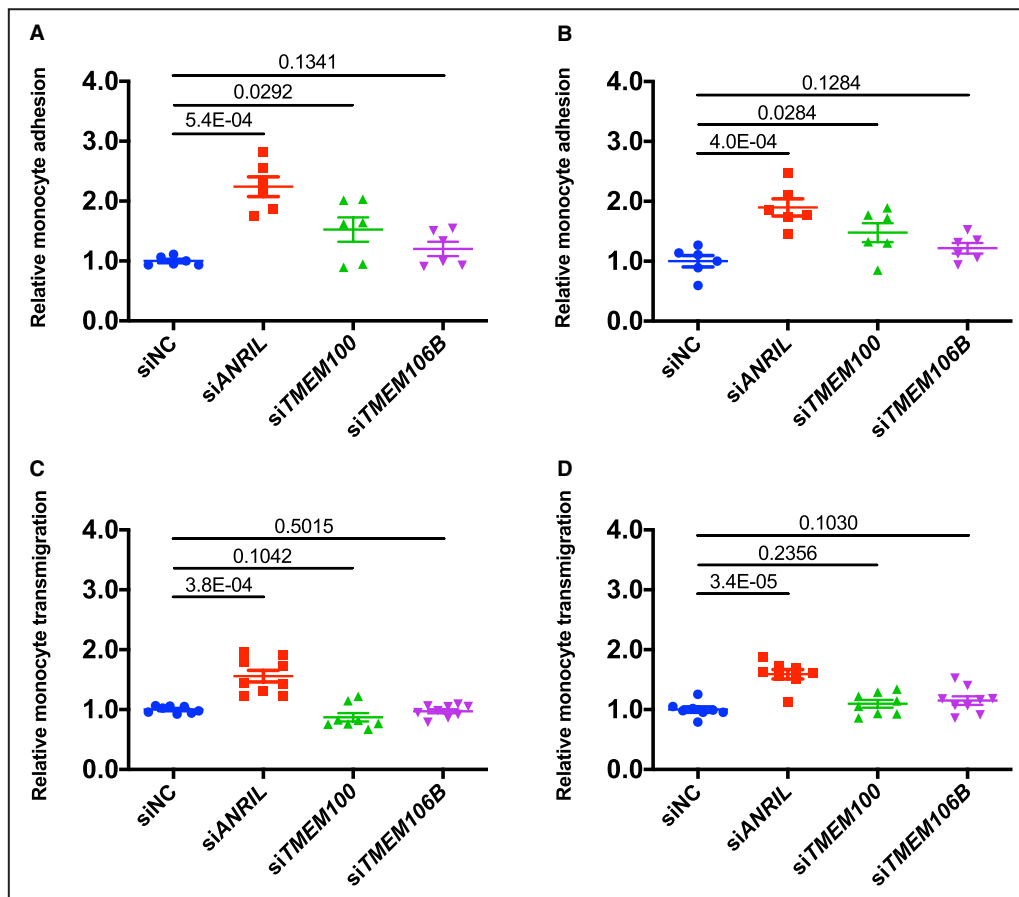


Figure 2. Analysis of the effect of knockdown of *TMEM100* or *TMEM106B* on monocyte adhesion to endothelial cells and transendothelial migration of monocytes.

A, Relative adhesion of monocytes to EA.hy926 cells transfected with small interfering (si)NC, siANRIL, siTMEM100, or siTMEM106B ($n=6$ samples/group; 3 wells/experiment with each experiment repeated again). **B**, Relative adhesion of monocytes to human coronary artery endothelial cells transfected with siNC, siANRIL, siTMEM100, or siTMEM106B ($n=6$ samples/group; 3 wells/experiment with each experiment repeated again). **C**, Relative transmigration of monocytes across a layer of EA.hy926 cells transfected with siNC, siANRIL, siTMEM100, or siTMEM106B ($n=9$ samples/group; 3 wells/experiment with each experiment repeated twice again). **D**, Relative transmigration of monocytes across human coronary artery endothelial cells transfected with siNC, siANRIL, siTMEM100, or siTMEM106B ($n=9$ samples/group; 3 wells/experiment with each experiment repeated twice again). Statistical analysis was performed using unpaired, 2-tailed Student t -tests. Si indicates small interfering.

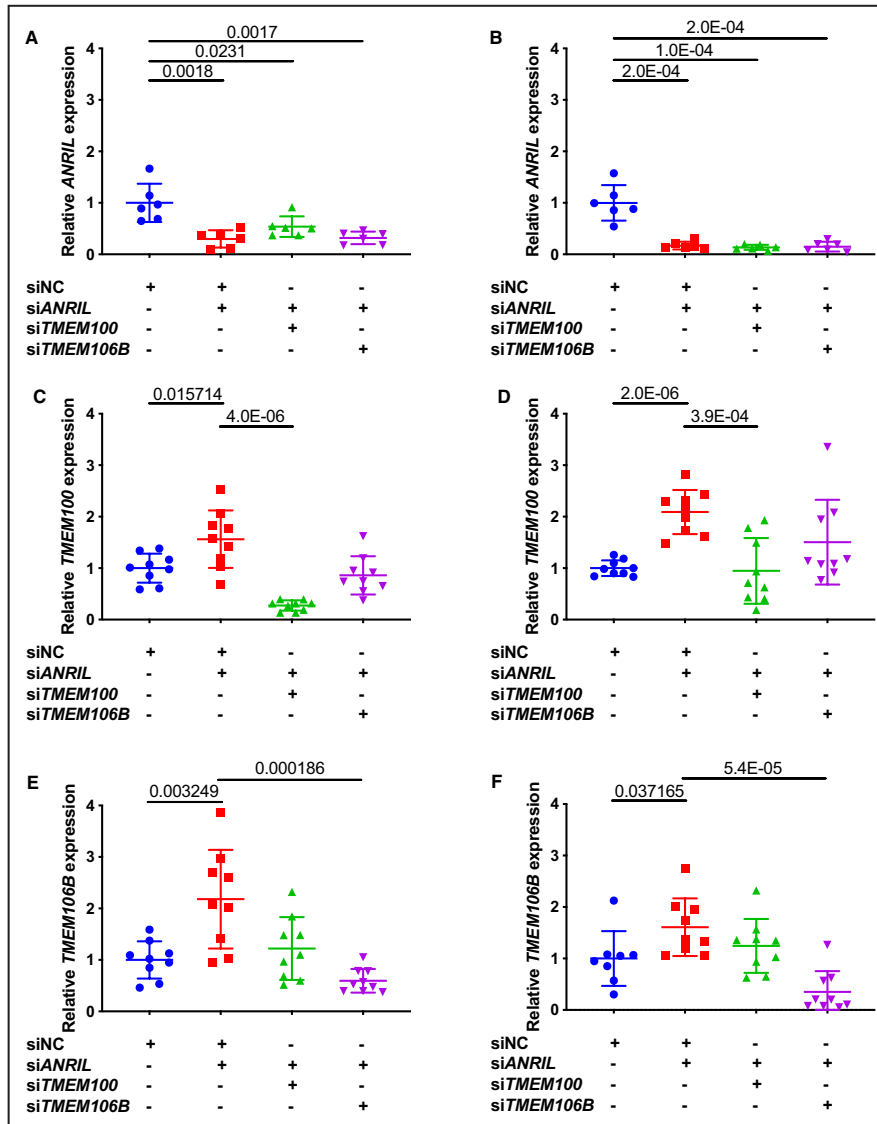


Figure 3. Real-time reverse transcription-polymerase chain reaction (RT-PCR) analysis of expression of *ANRIL*, *TMEM100*, and *TMEM106B* in endothelial cells (ECs) transfected with different siRNA.

A, Relative expression of *ANRIL* in EA.hy926 cells transiently co-transfected with different combinations of small interfering (si)NC (negative control siRNA), si*ANRIL*, si*TMEM100*, or si*TMEM106B* was quantified by quantitative RT-PCR (qRT-PCR) (n=6 samples/group; 3 wells/experiment with each experiment repeated again). **B**, Relative expression of *ANRIL* in human coronary artery endothelial cells transiently co-transfected with different combinations of siNC, si*ANRIL*, si*TMEM100*, or si*TMEM106B* (n=6 samples/group; 3 wells/experiment with each experiment repeated again) was quantified by qRT-PCR. **C**, Relative expression of *TMEM100* in EA.hy926 cells transiently co-transfected with different combinations of siNC, si*ANRIL*, si*TMEM100*, or si*TMEM106B* (n=9 samples/group; 3 wells/experiment with each experiment repeated twice again) was quantified by qRT-PCR. **D**, Relative expression of *TMEM100* in human coronary artery endothelial cells transiently co-transfected with different combinations of siNC, si*ANRIL*, si*TMEM100*, or si*TMEM106B* (n=9 samples/group; 3 wells/experiment with each experiment repeated twice again) was quantified by qRT-PCR. **E**, Relative expression of *TMEM106B* in EA.hy926 cells transiently co-transfected with different combinations of siNC, si*ANRIL*, si*TMEM100*, or si*TMEM106B* (n=9 samples/group; 3 wells/experiment with each experiment repeated twice again) was quantified by qRT-PCR. **F**, Relative expression of *TMEM106B* in human coronary artery endothelial cells transiently co-transfected with different combinations of siNC, si*ANRIL*, si*TMEM100*, or si*TMEM106B* (n=9 samples/group; 3 wells/experiment with each experiment repeated twice again) was quantified by qRT-PCR. Statistical analysis was performed using unpaired, 2-tailed Student *t*-tests. Si indicates small interfering.

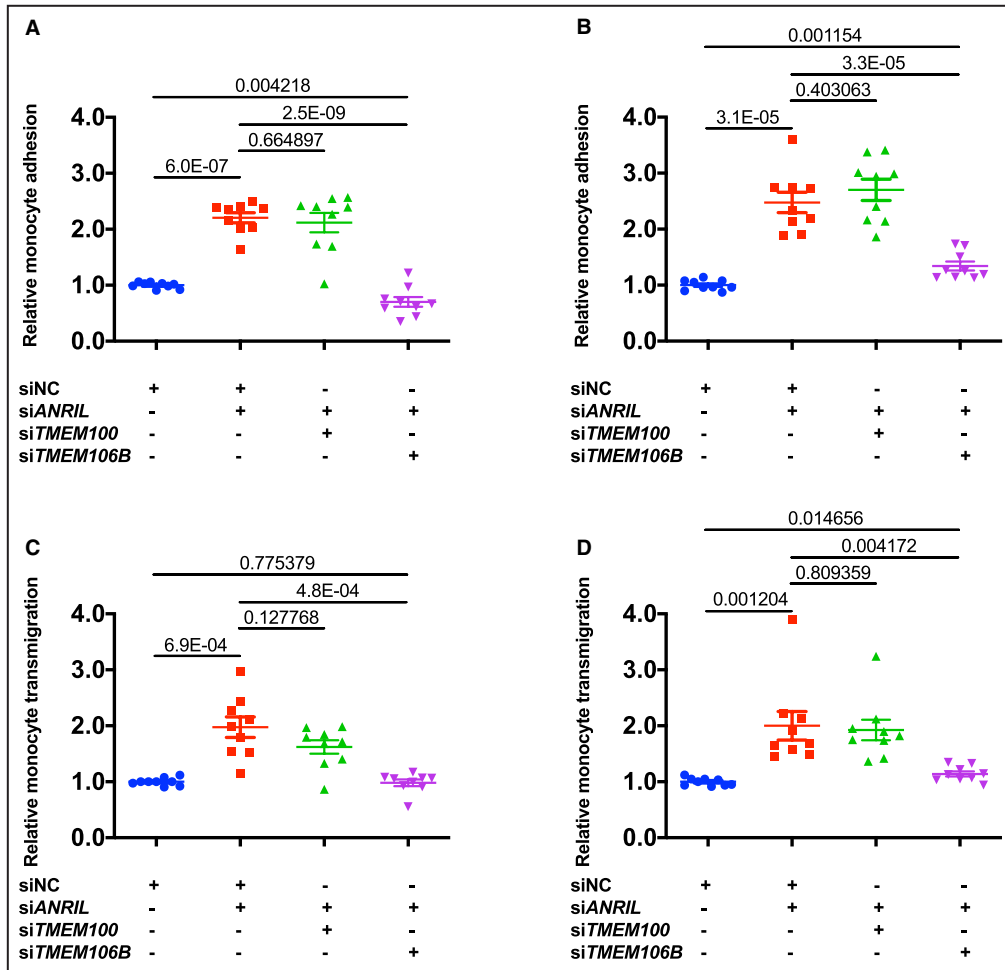


Figure 4. Knockdown of *TMEM106B*, but not *TMEM100*, reverses the effects of knockdown of *ANRIL* on monocyte adhesion to endothelial cells and transendothelial migration of monocytes. **A**, Relative adhesion of monocytes to EA.hy926 cells transiently co-transfected with different combinations of small interfering (si)NC (negative control siRNA), siANRIL, siTMEM100, or siTMEM106B (n=9 samples/group; 3 wells/experiment with each experiment repeated twice again). **B**, Relative adhesion of monocytes to human coronary artery endothelial cells transiently co-transfected with different combinations of siNC, siANRIL, siTMEM100, or siTMEM106B (n=9 samples/group; 3 wells/experiment with each experiment repeated twice again). **C**, Relative transmigration of monocytes across a layer of EA.hy926 cells transiently co-transfected with different combinations with siNC, siANRIL, siTMEM100, or siTMEM106B (n=9 samples/group; 3 wells/experiment with each experiment repeated twice again). **D**, Relative transmigration of monocytes across human coronary artery endothelial cells transiently co-transfected with different combinations with siNC, siANRIL, siTMEM100, or siTMEM106B (n=9 samples/group; 3 wells/experiment with each experiment repeated twice again). Statistical analysis was performed using unpaired, 2-tailed Student *t*-tests. Si indicates small interfering.

increased effect on EA.hy926 and HCAECs, whereas a positive control, *ANRIL* siRNA, showed a stronger effect on increasing monocyte adhesion to EA.hy926 and HCAECs (Figure 2A and 2B). On the other hand, knockdown of neither *TMEM100* nor *TMEM106B* in EA.hy926 and HCAECs showed any effect on transendothelial migration of monocytes although positive control *ANRIL* siRNA significantly increased transendothelial migration of monocytes (Figure 2C and 2D).

As *ANRIL* knockdown increased *TMEM100* and *TMEM106B* expression, we next examined whether

knockdown of *TMEM100* and *TMEM106B* could reverse the effects of *ANRIL* on ECs. We first confirmed that in EAhy926 and HCAECs co-transfected with *ANRIL* siRNA and *TMEM100* siRNA or *TMEM106B* siRNA showed successful knockdown of both *ANRIL* and *TMEM100* or knockdown of both *ANRIL* and *TMEM106B* (Figure 3A through 3F). Knockdown of *TMEM106B* effectively reversed the effect of *ANRIL* knockdown on monocyte adhesion to EA.hy926 (Figure 4A) and HCAECs (Figure 4B) and transendothelial migration of monocytes (Figure 4C and 4D). However, knockdown of *TMEM100*

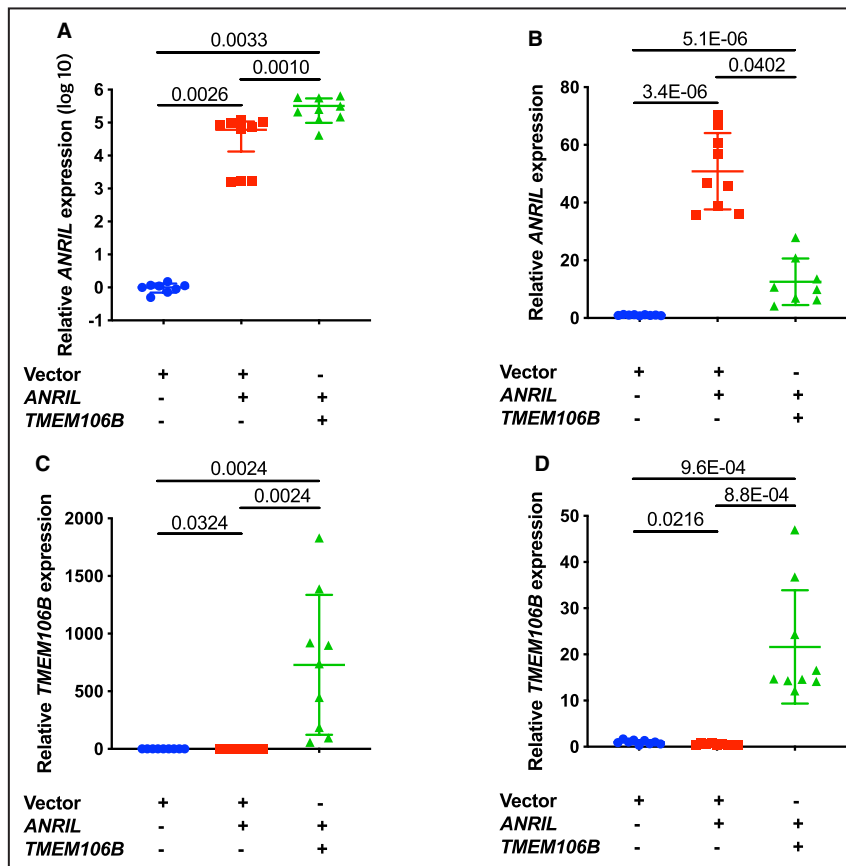


Figure 5. Overexpression of *TMEM106B* reverses the effects of *ANRIL* overexpression on monocyte adhesion to endothelial cells and transendothelial migration of monocytes.

A, Relative expression of *ANRIL* in a scale of log₁₀ in EA.hy926 cells transiently co-transfected with different combinations of pcDNA3.1, pcDNA3.1-*ANRIL*, or pcDNA3.1-*TMEM106B* (n=9 samples/group; 3 wells/experiment with each experiment repeated twice again). **B**, Relative expression of *ANRIL* in human coronary artery endothelial cells transiently co-transfected with different combinations of pcDNA3.1, pcDNA3.1-*ANRIL*, or pcDNA3.1-*TMEM106B* (n=9 samples/group; 3 wells/experiment with each experiment repeated twice again). **C**, Relative expression of *TMEM106B* in EA.hy926 transiently co-transfected with different combinations of pcDNA3.1, pcDNA3.1-*ANRIL*, or pcDNA3.1-*TMEM106B* (n=9 samples/group; 3 wells/experiment with each experiment repeated twice again). **D**, Relative expression of *TMEM106B* in human coronary artery endothelial cells transiently co-transfected with different combinations of pcDNA3.1, pcDNA3.1-*ANRIL*, or pcDNA3.1-*TMEM106B* (n=9 samples/group; 3 wells/experiment with each experiment repeated twice again). **E**, Relative adhesion of monocytes to EA.hy926 cells transiently co-transfected with different combinations of pcDNA3.1, pcDNA3.1-*ANRIL*, or pcDNA3.1-*TMEM106B* (n=9 samples/group; 3 wells/experiment with each experiment repeated twice again). **F**, Relative adhesion of monocytes to human coronary artery endothelial cells transiently co-transfected with different combinations of pcDNA3.1, pcDNA3.1-*ANRIL*, or pcDNA3.1-*TMEM106B* (n=9 samples/group; 3 wells/experiment with each experiment repeated twice again). **G**, Relative transmigration of monocytes across a layer of EA.hy926 cells transiently co-transfected with different combinations of pcDNA3.1, pcDNA3.1-*ANRIL*, or pcDNA3.1-*TMEM106B* was quantified (n=9 samples/group; 3 wells/experiment with each experiment repeated twice again). **H**, Relative transmigration of monocytes across human coronary artery endothelial cells transiently co-transfected with different combinations of pcDNA3.1, pcDNA3.1-*ANRIL*, or pcDNA3.1-*TMEM106B* (n=9 samples/group; 3 wells/experiment with each experiment repeated twice again). Statistical analysis was performed using unpaired, 2-tailed Student *t*-tests.

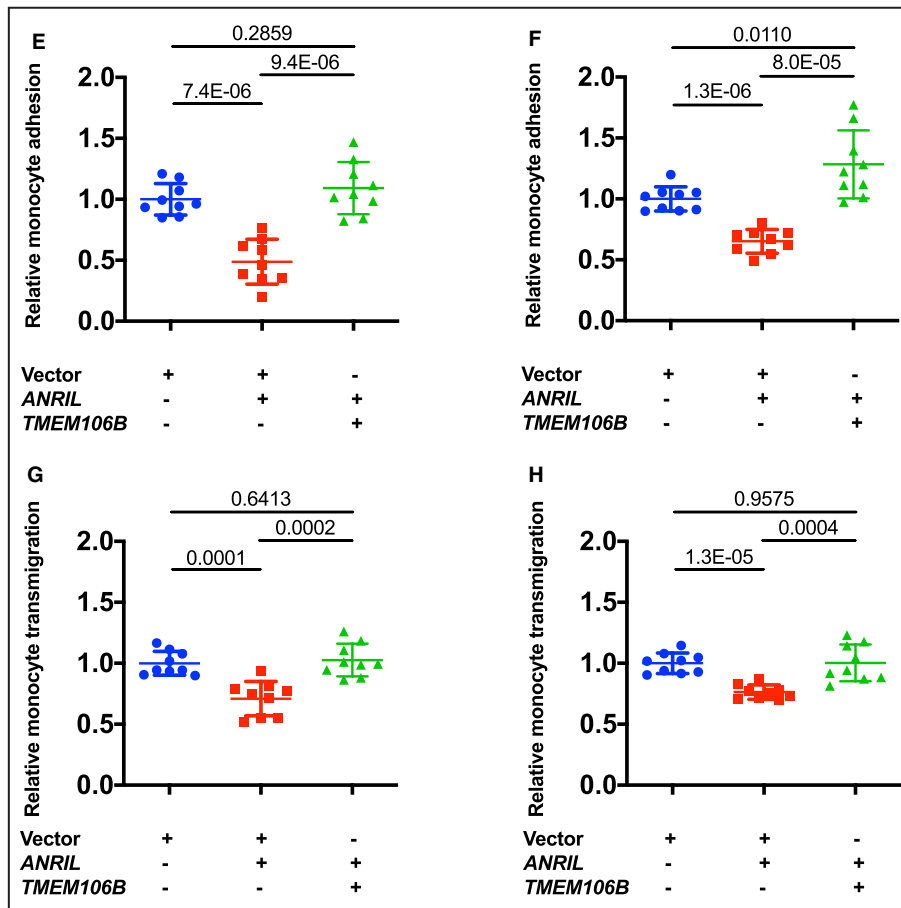


Figure 5. Continued

did not have any significant impact on the effects of *ANRIL* knockdown on monocyte adhesion to ECs or transendothelial migration of monocytes in EA.hy926 (Figure 4A through 4D). These data suggest that *ANRIL* knockdown affects EC functions relevant to atherosclerosis by upregulating the expression of *TMEM106B*, but not *TMEM100*.

Overexpression of *TMEM106B* Rescues *ANRIL* Overexpression Phenotype of Endothelial Cells Involved in Atherosclerosis

We also characterized the effect of *TMEM106B* overexpression on function of *ANRIL* overexpression in ECs. We previously reported that overexpression of *ANRIL* transcript DQ485454 significantly reduced monocyte adhesion to ECs and transendothelial migration of monocytes.⁵ EA.hy926 cells and HCAECs were co-transfected with pcDNA3.1-*ANRIL* and pcDNA3.1-*TMEM106B*, and *ANRIL* and *TMEM106B* were successfully co-expressed (Figure 5A through 5D). Overexpression of *ANRIL* significantly decreased monocyte adhesion to EA.hy926 cells and

HCAECs and transendothelial migration of monocytes, however, the effects were fully reversed by overexpression of *TMEM106B* (Figure 5E through 5H). Overexpression of *TMEM106B* alone (eg without overexpression of *ANRIL*) did not show much effect on monocyte adhesion to EA.hy926 cells and HCAECs and transendothelial migration of monocytes (Figure 6A through 6H). These data suggest that overexpression of *TMEM106B* fully reverses the inhibitory function of *ANRIL* in monocyte adhesion to ECs and transendothelial migration of monocytes involved in atherosclerosis.

TMEM106B, But Not *TMEM100*, is Upregulated in CAD Coronary Arteries

We found that *TMEM106B* is upregulated in CAD coronary arteries, which is consistent with its key role in the pathogenesis of CAD. We assessed the expression level of *TMEM106B* in coronary arteries from CAD patients with coronary artery stenosis of 40% to 100% as compared with those from the age-, sex-, and race-matched non-CAD control subjects (Table). As previously reported,⁵ the expression

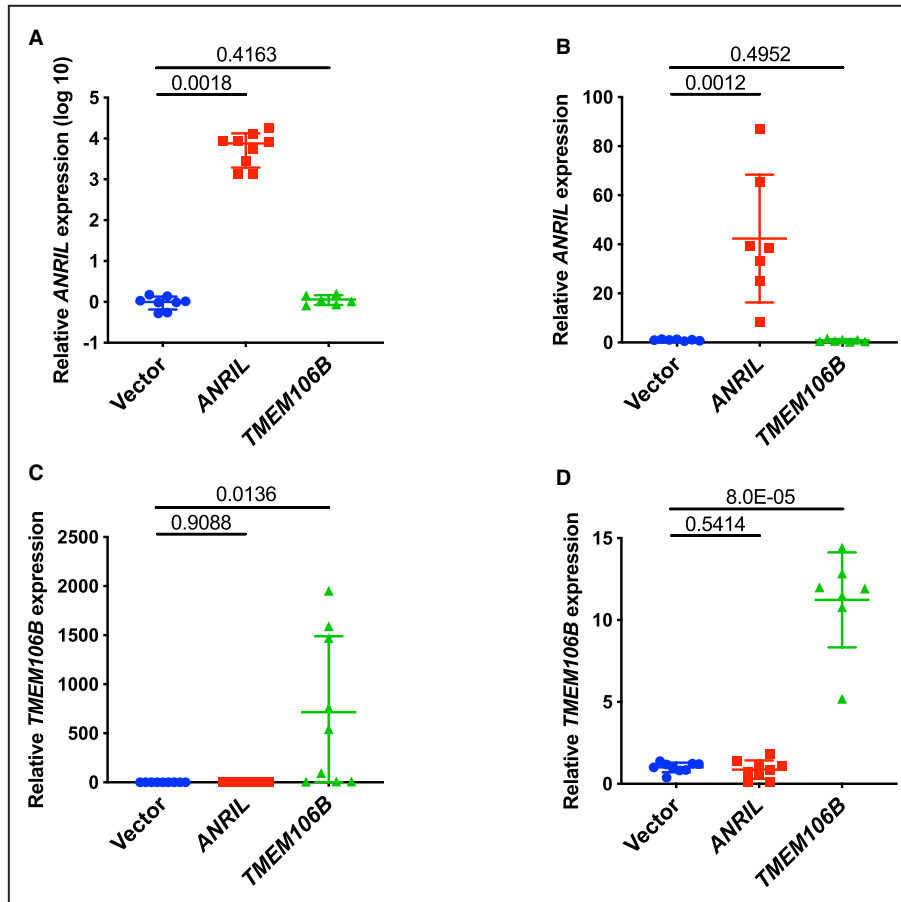


Figure 6. Overexpression of *TMEM106B* alone does not have any effects on monocyte adhesion to endothelial cells and transendothelial migration of monocytes.

A, Relative expression of *ANRIL* in a scale of \log_{10} in EA.hy926 cells transiently transfected with pcDNA3.1, pcDNA3.1-*ANRIL*, or pcDNA3.1-*TMEM106B* (n=9 samples/group; 3 wells/experiment with each experiment repeated twice again). **B**, Relative expression of *ANRIL* in human coronary artery endothelial cells transiently transfected with pcDNA3.1, pcDNA3.1-*ANRIL*, or pcDNA3.1-*TMEM106B* (n=9 samples/group; 3 wells/experiment with each experiment repeated twice again). **C**, Relative expression of *TMEM106B* in EA.hy926 cells transiently transfected with pcDNA3.1, pcDNA3.1-*ANRIL*, or pcDNA3.1-*TMEM106B* (n=9 samples/group; 3 wells/experiment with each experiment repeated twice again). **D**, Relative expression of *TMEM106B* in human coronary artery endothelial cells transiently transfected with pcDNA3.1, pcDNA3.1-*ANRIL*, or pcDNA3.1-*TMEM106B* (n=9 samples/group; 3 wells/experiment with each experiment repeated twice again). **E**, Relative adhesion of monocytes to EA.hy926 cells transfected with pcDNA3.1, pcDNA3.1-*ANRIL*, or pcDNA3.1-*TMEM106B* (n=6 samples/group; 3 wells/experiment with each experiment repeated again). **F**, Relative adhesion of monocytes to HCAECs transfected with pcDNA3.1, pcDNA3.1-*ANRIL*, or pcDNA3.1-*TMEM106B* (n=6 samples/group; 3 wells/experiment with each experiment repeated again). **G**, Relative transmigration of monocytes across a layer of EA.hy926 cells transfected with pcDNA3.1, pcDNA3.1-*ANRIL*, or pcDNA3.1-*TMEM106B* (n=6 samples/group; 3 wells/experiment with each experiment repeated again). **H**, Relative transmigration of monocytes across HCAECs transfected with pcDNA3.1, pcDNA3.1-*ANRIL*, or pcDNA3.1-*TMEM106B* (n=9 samples/group; 3 wells/experiment with each experiment repeated twice again). Statistical analysis was performed using unpaired, 2-tailed Student *t*-tests.

level of *ANRIL* (DQ485454) was significantly lower in CAD patients by >100-fold compared with that of the age-matched healthy controls ($P=0.026$) (Figure 7A). Interestingly, *TMEM106B* expression was significantly increased by more than 2-fold in CAD coronary

arteries compared with control coronary arteries ($P=0.0006$) (Figure 7B). However, there was no significant difference for the expression level of *TMEM100* between CAD coronary arteries and control coronary arteries (Figure 7C). Together, the data are consistent

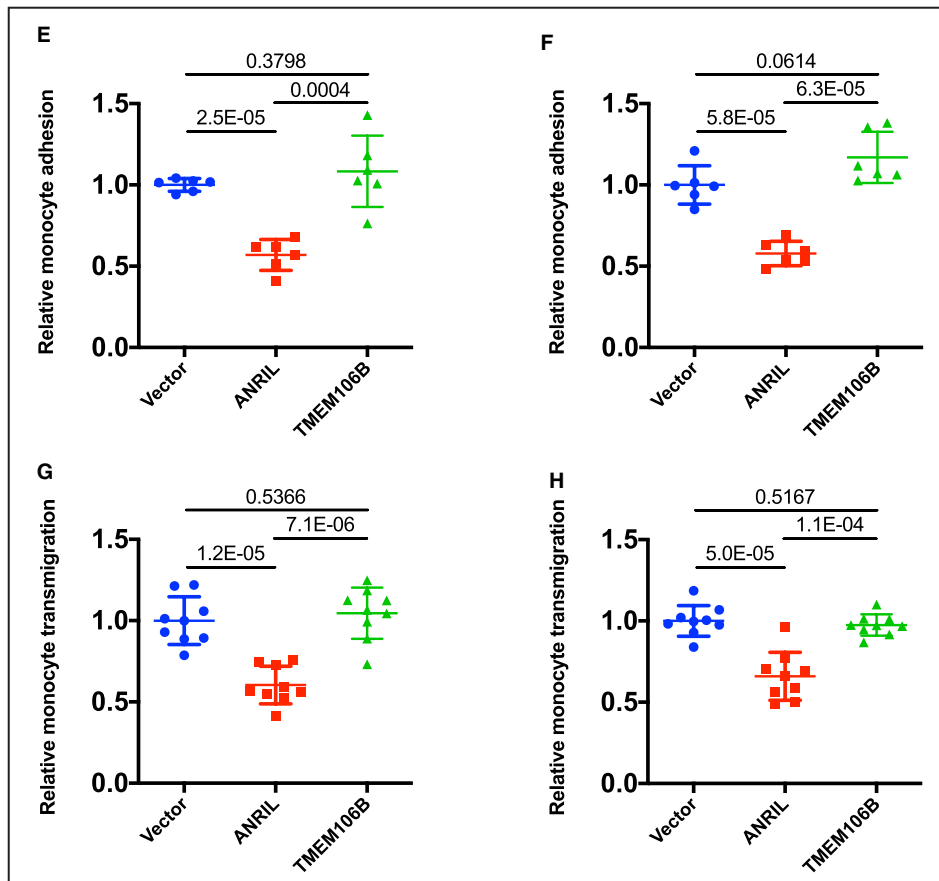


Figure 6. Continued

with earlier functional data showing that overexpression of *ANRIL* showed a protective effect on atherosclerosis, ie, reduced monocyte adhesion to ECs and transendothelial migration of monocytes, however, the effect was fully antagonized by overexpression of *TMEM106B*, but not *TMEM100*.

***TMEM100B* Does Not Affect the Expression Level of *CDKN2A*, *CDKN2B*, or *MTAP* Genes at the 9p21.3 CAD Locus**

We recently reported that knockdown of *ANRIL* (DQ485454) significantly decreased the expression level of *CDKN2A* and *CDKN2B* but not *MTAP* at the 9p21.3 CAD locus, whereas overexpression of *ANRIL* significantly increased the expression level of *CDKN2B* but not *CDKN2A* and *MTAP* in HCAECs.⁵ We performed a similar study for *TMEM106B* (Figure 8). Overexpression of *TMEM106B* did not significantly affect the expression level of *CDKN2A*, *CDKN2B*, or *MTAP* in HCAECs (Figure 8A). Knockdown of *TMEM106B* by siRNA did not significantly affect the expression level of *CDKN2A*, *CDKN2B*, or *MTAP* in HCAECs (Figure 8B). Therefore, although *ANRIL*

regulates the expression of *CDKN2A* or *CDKN2B*, neither overexpression nor knockdown of *TMEM106B* had any significant effect on the expression level of *CDKN2A*, *CDKN2B*, or *MTAP* in HCAECs.

Genomic Variants in *TMEM106B* are Significantly Associated With Risk of CAD

Because *TMEM106B* regulates the function of *ANRIL* on EC functions involved in atherosclerosis, we hypothesized that genomic variants in *TMEM106B* are associated with risk of CAD. We used 2 large existing GWAS data sets (CADRDloGRAMplusC4D and GeneATLAS [phenotype code: I20-I25]) to determine the association between genomic variants in a 100 kb genomic region flanking *TMEM106B* and CAD. A total of 887 variants in the *TMEM106B* region were selected for a meta-analysis of 636 539 samples. One variant, rs11509880 located in intron 4 of *TMEM106B*, was found to be robustly associated with CAD ($P=1.9\times 10^{-8}$, odds ratio=1.03, 95% CI=1.02–1.05) (Figure 9A). No significant association with CAD was detected for genomic variants in and around *CLIP1*, *EZR*, and *LYVE1*, 3 genes previously

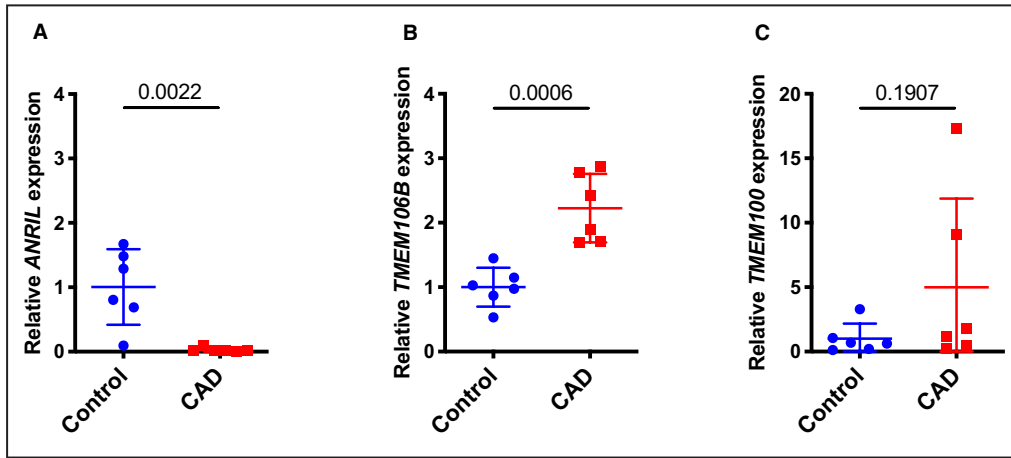


Figure 7. *TMEM106B*, but not *TMEM100*, is significantly upregulated in coronary arteries from coronary artery disease (CAD) patients and correlated with downregulation of *ANRIL*.

A. Relative expression levels of *ANRIL* as determined by quantitative reverse transcription-polymerase chain reaction from coronary artery tissues from CAD patients and the age-matched non-CAD individuals (n=6 tissues or study subjects/group). **B.** Relative expression levels of *TMEM106B* as determined by quantitative reverse transcription-polymerase chain reaction from coronary artery tissues from CAD patients and the age-matched non-CAD individuals (n=6 tissues or study subjects/group). **C.** Relative expression levels of *TMEM100* as determined by qRT-PCR from coronary artery tissues from CAD patients and the age-matched non-CAD individuals (n=6 tissues or study subjects/group). Statistical analysis was performed using unpaired, 2-tailed Student *t* tests.

shown to be involved in regulation of *ANRIL* functions (data not shown). These data suggest that genomic variants in *TMEM106B*, but not in other *ANRIL* downstream genes *TMEM100*, *CLIP1*, *EZR*, and *LYVE1*, are significantly associated with risk of CAD.

Significant Gene-Gene Interaction Between the *ANRIL* Locus and the *TMEM106B* Locus

Because *ANRIL* negatively regulates the expression of *TMEM106B*, and *TMEM106B* antagonizes the function

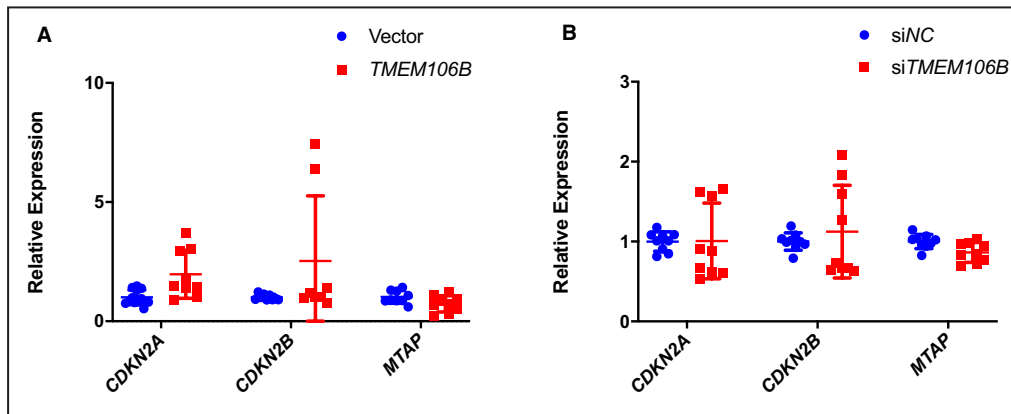


Figure 8. Neither overexpression nor knockdown of *TMEM106B* affects the expression of the *CDKN2A*, *CDKN2B*, and *MTAP* genes at the 9p21.3 CAD locus.

A. Relative expression level of *CDKN2A*, *CDKN2B*, and *MTAP* as determined by quantitative reverse transcription-polymerase chain reaction analysis from human coronary artery endothelial cells transiently transfected with either pcDNA3.1 vector or pcDNA-*TMEM106B* (n=9 samples/group; 3 wells/experiment with each experiment repeated twice again). **B.** Relative expression level of *CDKN2A*, *CDKN2B*, and *MTAP* in human coronary artery endothelial cells transiently transfected with either small interfering NC or small interfering *TMEM106B* as determined by quantitative reverse transcription-polymerase chain reaction (n=9 samples/group; 3 wells/experiment with each experiment repeated twice again). Statistical analysis was performed using unpaired, 2-tailed Student *t*-tests. Si indicates small interfering.

of *ANRIL* in ECs, we hypothesized that genetically, the *ANRIL* locus may interact with the *TMEM106B* locus in exerting an epistasis effect on CAD. To test this hypothesis, we selected genetic variant rs2383207 in the *ANRIL* locus for the analysis, which is a tag single nucleotide polymorphism for the ≈ 60 kb CAD haplotype at 9p21 (Figure 9B). For the *TMEM106B* locus, we selected variant rs3807865 (Figure 9A), which shows a significant and strong eQTL (Expression Quantitative Trait Locus) for *TMEM106B* and is located in a strong H3K27Ac and DNase cluster site. Analysis of the genotyping data for I20-I25 Ischemic heart diseases in UK Biobank using a logistic regression model detected a significant epistatic interaction between the 2 variants when both are in the homozygous state (odds ratio=1.16, $P=0.0087$)

(Figure 9C). These results suggest that the *ANRIL* locus and the *TMEM106B* locus genetically interact with each other, which is consistent with the finding of functional interaction between the 2 genes.

Validation of the Forward Genetic Approach in Identification of the Second Pair of Gene-Gene Interaction Between *ADTRP* and *MIA3* Loci for CAD

All data above suggest that we have developed a novel forward genetic approach that is effective in identifying epistasis involved in common human diseases. It consists of multiple steps that combine statistical and functional approaches to functionally characterize

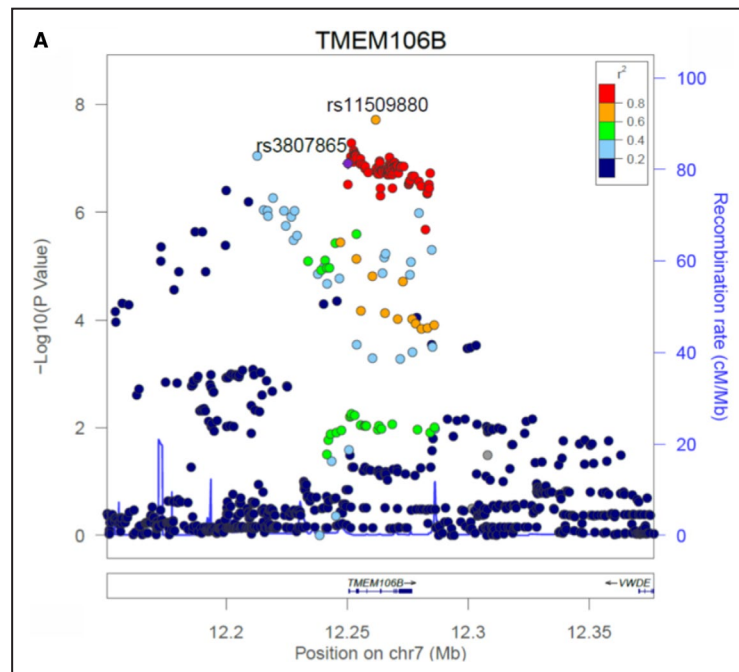


Figure 9. Genetic evidence for epistasis involving the *ANRIL* and *TMEM106B* GWAS (genome-wide association studies) loci for coronary artery disease (CAD).

A, Regional association plot of *TMEM106B* from a meta-analysis of 2 large CAD GWAS data sets. The recombination rate as plotted in centi-morgan (cM)/Mb (a million base pair) and genetic association as plotted in the scale of $-\log_{10}$ are shown. Color of the individual dot indicates the linkage disequilibrium between the lead single nucleotide polymorphism (purple dot) and other single nucleotide polymorphisms. The displayed linkage disequilibrium data and recombination rates are based on the European population in the 1000 Genome database. **B**, Regional association plot of *ANRIL* from a meta-analysis of 2 large CAD GWAS data sets. **C**, Significant genetic interaction between *ANRIL* variant rs2383207 and *TMEM106B* variant rs3807865 in 343 145 unrelated samples in UK Biobank. Genetic interactions between 2 genes were assessed using a logistic regression model, in which 2 main effects of each gene and 4 interactions between genes were modeled. The non-risk homozygote was set as the reference for each gene. Statistical analysis was performed as described in Methods section. OR indicates odds ratio; P , P value from the logistic regression model with adjustment of covariates.

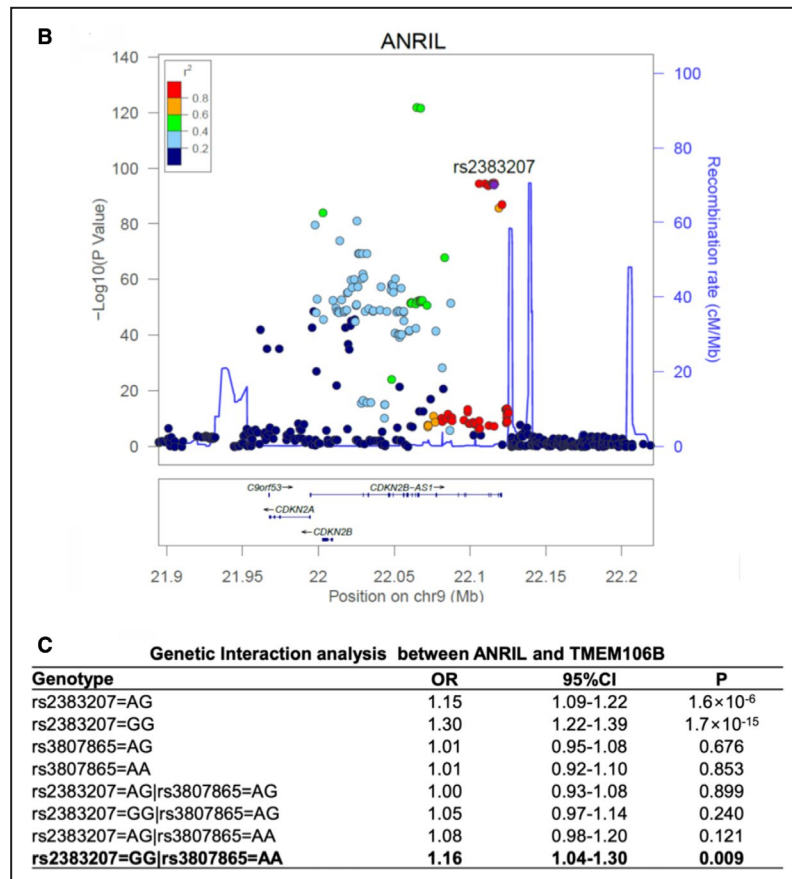


Figure 9. Continued

GWAS variants. As proof of principle, we combined information from global gene expression profiling, functional interactions, and genetic interactions to robustly identify the gene-gene interaction between the *ANRIL* locus and the *TMEM106B* locus involved in CAD. To generalize the multi-stage forward genetic approach, we characterize 2 other GWAS loci for CAD, the *ADTRP* locus^{12,13} on chromosome 6p24.1 and the *MIA3* locus^{14,15} on 1q41, both of which were identified also by GWAS for CAD. We previously reported the functional interaction between *ADTRP* and *MIA3* (also referred to as *TANGO1*).²⁶ *ADTRP* is involved in endothelial cell proliferation, migration, cell cycle and apoptosis regulation, primitive myelopoiesis, definitive hematopoiesis, and vascular development.^{25,31,32} *MIA3* is involved in the transport of large cargos such as collagen into membrane-bound carriers and export from the endoplasmic reticulum.³³ Our global gene expression microarray analysis with knockdown of *ADTRP* expression identified *MIA3* as one of the downstream genes. Mechanistic studies revealed that *ADTRP* positively regulates expression of *MIA3* by upregulating *PIK3R3* and activating AKT.²⁶ Knockdown of *ADTRP* expression significantly increased oxidized low-density lipoprotein-mediated monocyte adhesion to endothelial

cells and transendothelial migration of monocytes, however, the effects were reversed by overexpression of *MIA3* overexpression.²⁶ Moreover, we found that *MIA3* negatively regulates the expression level of *ADTRP* in both HepG2 cells (Figure 10A through 10D) and EA.hy926 endothelial cells (Figure 10E and 10F). Therefore, functional regulatory interaction between *ADTRP* and *MIA3* was identified. Because the large data set at UK Biobank recently becomes available, we tested the genetic interaction between the 2 genes using 2 genomic variants showing the most significant association with CAD, rs6903956 in *ADTRP*¹² and rs17465637 in *MIA3*¹⁵ (Figure 11A and 11B). Interestingly, we observed a significant epistatic interaction between rs6903956 in *ADTRP* and rs17465637 in *MIA3* (odds ratio=0.80, $P=0.005$) (Figure 11C).

DISCUSSION

One interesting finding from this study is that molecular characterization of one susceptibility gene for CAD from GWAS (ie, *ANRIL*) leads to the genetic identification of another CAD susceptibility gene (ie, *TMEM106B*). Most GWAS for common human diseases are almost exhausted in identifying additional new susceptibility

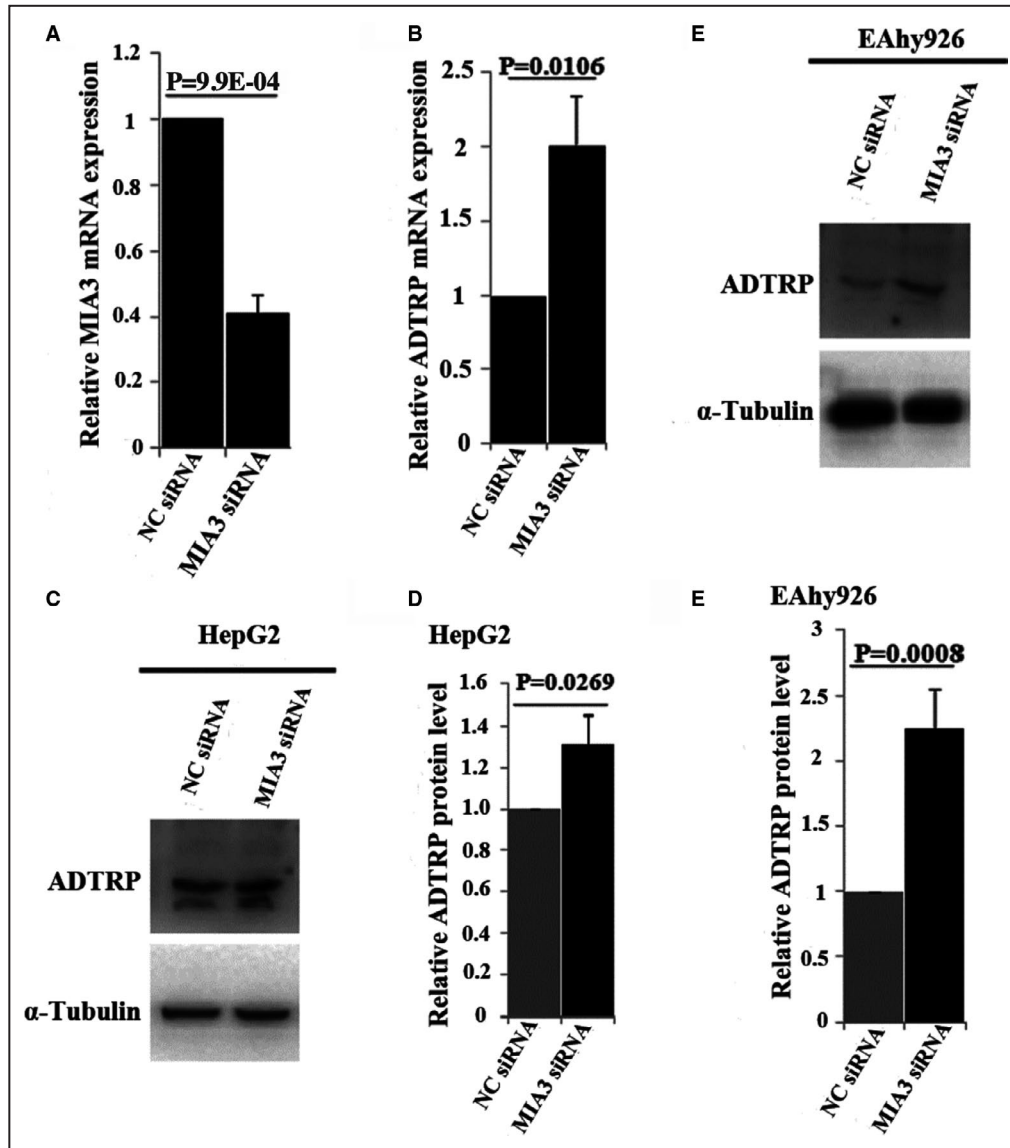


Figure 10. *MIA3* negatively regulates the expression level of *ADTRP*.

A, Real-time RT-PCR analysis showing that *MIA3* small interfering (si)RNA significantly reduces its expression. **B**, Real-time RT-PCR analysis showing that *MIA3* siRNA significantly increases the expression of *ADTRP* mRNA. **C**, Western blot analysis showing that *MIA3* siRNA significantly increases the expression of the *ADTRP* protein in HepG2 cells. **D**, Quantification of Western blot images in (**C**) and statistical analysis showing that *MIA3* siRNA significantly increases the expression of the *ADTRP* protein in HepG2 cells. **E**, Western blot analysis showing that *MIA3* siRNA significantly increases the expression of the *ADTRP* protein in EA.hy926 ECs. **F**, Quantification of Western blot images in **E** and statistical analysis showing that *MIA3* siRNA significantly increases the expression of the *ADTRP* protein in EA.hy926 ECs. α -Tubulin was used as loading control for Western blot analysis. $n=3$ samples/group from 3 independent experiments. Statistical analysis was performed using unpaired, 2-tailed Student t tests. Si indicates small interfering.

genes with ever increasing sample sizes of close to a million study subjects. It will be difficult to further increase the sample size to find new susceptibility variant or loci. The combination of functional characterization of existing susceptibility genes for downstream genes and follow-up genetic association analysis, as demonstrated in this study, may be a viable strategy to identify some new susceptibility genes in the future.

Among the 2 genes upregulated by knockdown of *ANRIL* expression (*TMEM100* and *TMEM106B*), it was surprising that knockdown of *TMEM100* did not impact the effects of *ANRIL* knockdown on monocyte adhesion to EA.hy926 cells and HCAECs or transendothelial migration of monocytes (Figure 4). Consistent with the finding, we did not find significant genetic association between *TMEM100*

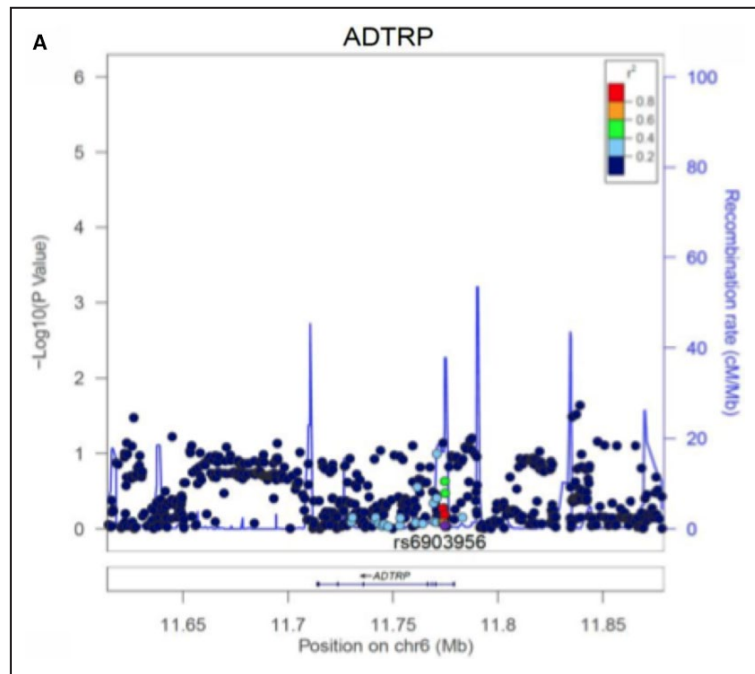


Figure 11. Genetic evidence for epistasis involving the *ADTRP* and *MIA3* GWAS (genome-wide association studies) loci for coronary artery disease (CAD).

A, Regional association plot of *ADTRP* from a meta-analysis of 2 large CAD GWAS data sets. **B**, Regional association plot of *MIA3* from a meta-analysis of 2 large CAD GWAS data sets. The recombination rate as plotted in cM/Mb and genetic association as plotted in the scale of $-\log_{10}$ are shown. Color of the individual dot indicates the linkage disequilibrium between the lead single nucleotide polymorphism (purple dot) and other single nucleotide polymorphisms. The displayed linkage disequilibrium data and recombination rates are based on the European population in the 1000 Genome database. **C**, Significant genetic interaction between *ADTRP* variant rs6903956 and *MIA3* variant rs17465637 in 343 145 unrelated samples in UK Biobank. Genetic interactions between 2 genes were assessed using a logistic regression model, in which 2 main effects of each gene and 4 interactions between genes were modeled. The non-risk homozygote was set as the reference for each gene. Statistical analysis was performed as described in Methods section. OR indicates odds ratio; *P*, *P* value from the logistic regression model with adjustment of covariates.

variants and CAD (Figure 9) or deregulation in CAD contrary arteries as compared with control arteries (Figure 8). *TMEM100* was found to be an upregulated gene by BMP9 (Bone Morphogenic Protein 9) and BMP10 (Bone Morphogenic Protein 10) through their ALK1 receptor, all of which regulate embryonic vascular development.⁶ Global knockout or EC-specific knockout mice for *TMEM100* showed abnormal differentiation of arterial endothelium and defects of vascular morphogenesis during embryogenesis⁶ and defective maintenance of vascular integrity and various vascular abnormalities during the adult stage.⁸ Despite these interesting roles of *TMEM100* in endothelial differentiation and vascular development, it showed only a modest effect on monocyte adhesion to ECs, and no effect on

transendothelial migration of monocytes or *ANRIL* functions in endothelial cells (Figure 4).

In contrast to *TMEM100*, we found that *TMEM106B* was required for the functional effects of *ANRIL* knockdown because the increased monocyte adhesion to EA.hy926 cells and HCAECs or transendothelial migration of monocytes induced by *ANRIL* knockdown disappeared when *TMEM106B* expression was also knocked down (Figure 4). We also showed that the expression level of *TMEM106B* was significantly higher by 2-fold in coronary arteries from CAD patients than from age-matched controls (Figure 7B). *TMEM106B* was shown to play a role of regulating lysosomal morphology, size, trafficking, and function.^{9–11,34} Knockout of *TMEM106B* in mice caused reduction of several lysosomal enzymes.³⁴

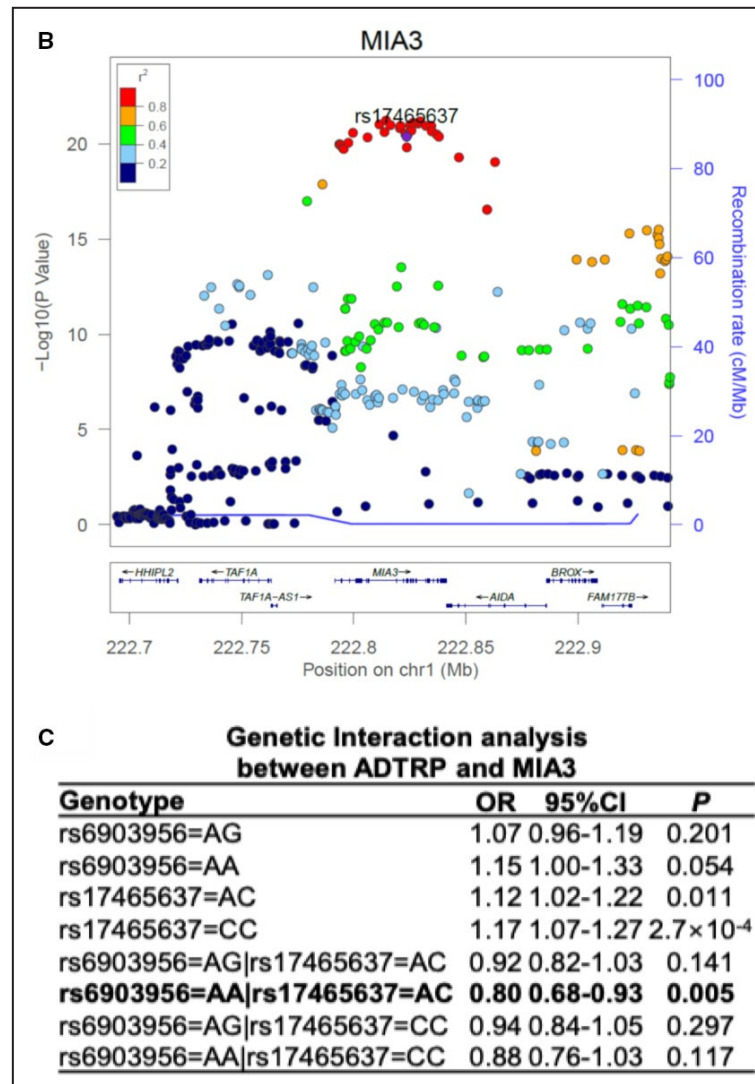


Figure 11. Continued

Overexpression of *TMEM106B* was shown to induce enlargement of lysosomes and a reduction in lysosome numbers, and caused a defect in the later stages of late endosome/lysosome fusion or lysosomal degradation.¹¹ Enlarged lysosomes may trap more cholesterol inside lysosomes, and lysosomal cholesterol accumulation was hypothesized to be involved in the development of inflammation during atherosclerosis.³⁵ In macrophages, lipids were mostly deposited in lysosomal organelles, and free cholesterol efflux from lysosomes was inhibited by *CD38* knockout, which leads to lysosomal cholesterol accumulation in macrophages and development of atherosclerosis in mice.³⁶ Moreover, macrophages isolated from atherosclerotic plaques showed dysfunction of lysosomes, and increased lysosome biogenesis in macrophages had an anti-atherogenic effect.^{37,38} It should be interesting to investigate whether the *ANRIL-TMEM106B* regulatory

network plays a role in free cholesterol efflux from lysosomes in macrophages in the future. Similarly, it should be interesting to characterize whether lysosome dysfunction plays a role in endothelial function such as monocyte adhesion to ECs and transendothelial migration of monocytes and to define the underlying molecular mechanism. Enlarged lysosomes may trap more cholesterol and lipids and cause inflammation, which may promote monocyte adhesion to ECs and transendothelial migration of monocytes.

The molecular mechanism by which *ANRIL* regulates the expression of *TMEM106B* and other downstream target genes in endothelial cells is not clear. *ANRIL* was reported to interact with the components of PRC1/2 such as EZH2, SUZ12, and CBX7 to facilitate the recruitment of the chromatin-modifying complex to promoter/regulatory regions, which can then regulate expression of adjacent genes.³⁹⁻⁴² *ANRIL* was also found to act as a sponge for some microRNAs in regulating expression

of downstream genes in nasopharyngeal carcinoma (let-7a),⁴³ lipopolysaccharide-induced inflammatory injury of HK-2 cells (miR-9),⁴⁴ hypoxia-induced injury in H9C2 cells (miR-7-5p/SIRT1),⁴⁵ oxygen and glucose deprivation-induced injury in PC-12 cells (miR-127/Mcl-1),⁴⁶ lipopolysaccharides- and pyrrolidine dithiocarbamate-treated endothelial cells (miR-181b/NF- κ B),⁴⁷ cell senescence of vascular smooth muscle cells (miR-181a/Sirt1),⁴⁸ and wound healing in diabetes mellitus (miR-181a/Prox1).⁴⁹ One or more of these molecular regulatory mechanisms may be used by *ANRIL* to regulate the expression of *TMEM106B* and other downstream target genes in endothelial cells, although we cannot exclude the possibility of other novel mechanisms. Future studies will focus on identification of molecular mechanisms by which *ANRIL* regulates *TMEM106B* and other genes involved in the pathogenesis of CAD.

Although GWAS have identified >150 genomic loci associated with CAD and MI,³ identification of the causal gene(s) under each locus and functional characterization of causal genes are challenging. The data from this study further confirm the notion from us and others that *ANRIL* is the causal gene for CAD at the 9p21.3 locus.^{4,5} Moreover, our data suggest that *TMEM106B* is the causal gene at the 7q21.11 CAD locus (Figure 9A).

Epistasis has been poorly characterized in human diseases because even the largest databases for CAD such as UK Biobank and C4DGRAMplusC4D may not have a sufficient power for a successful genome-wide gene-gene interaction study to satisfy the genome-wide significance. This is because of 2 major limitations. First, the number of tests for genome-wide gene-gene interaction studies will be exponential as compared with GWAS and poses an enormous challenge for correction for multiple testing. Second, the frequencies of rare genotypes may be too low to do reliable testing for gene-gene interactions, particularly for genomic variants with moderate or low minor allele frequencies. Our study provides a potential strategy for detecting epistasis for human diseases despite the fact that it has low throughput and is labor intensive. The strategy consists of several key steps: (1) selection of a GWAS variant or locus, (2) identification of a candidate causal gene based on bioinformatic analysis and existing genetic and biological data and functional validation, (3) identification of downstream genes for the candidate causal gene by expression microarrays or RNAseq, (4) functional rescue studies between the candidate causal gene and each downstream gene to identify the gene pairs showing functional interaction, and (5) genetic association between the gene pairs showing functional interaction. Identification of epistasis provides significant insights into the genetic architecture of common human diseases, and could have a

far-reaching impact on recent advances on exploration of polygenic risk scores, which are emerging as potentially powerful biomarkers to predict the risk to develop different human diseases.

Detailed analysis suggests that the type of gene-gene interaction between *ANRIL* and *TMEM106B* belongs to “negative epistasis”,⁵⁰ whereas the epistatic interaction between *ADTRP* and *MIA3* belongs to “sign epistasis”.⁵¹ The 2 different types of epistasis may result from distinctly different gene regulatory patterns underlying each pair of GWAS genes. In the first case of *ANRIL-TMEM106B* interaction, *ANRIL* negatively regulates the expression of *TMEM106B*, whereas *TMEM106B* did not have any effect on the expression of *ANRIL* (Figure 1A through 1F). Since the effect of *TMEM106B* on CAD is masked by or depends on *ANRIL*, the 2 genes together result in a reduced disease risk because of negative epistasis. In the case of *ADTRP-MIA3* interaction, *ADTRP* positively regulates the expression of *MIA3*,²⁶ however, we showed here that *MIA3* negatively regulated the expression of *ADTRP* (Figure 10). Our previous studies showed that the risk allele of *ADTRP* was correlated with the decreased *ADTRP* expression level,¹² which could lead to downregulation of *MIA3* and abnormal EC functions associated with CAD.²⁶ However, the effect of the *ADTRP* risk allele (or downregulation of *ADTRP*) on CAD may be weakened or reversed by downregulation of *MIA3*, which could upregulate the expression of *ADTRP*. Thus, the observed sign epistasis between *ADTRP* and *MIA3* may arise from the bidirectional negative feedback gene regulation. Identification of different types of epistasis, for example, negative epistasis and sign epistasis as shown here, among different GWAS genes is critical to a better understanding of polygenic contribution in CAD and other complex diseases. More importantly, as studies on polygenic risk scores for disease risk stratification and prognosis become popular these days, a careful consideration of epistasis is needed because different types of epistasis can have an important effect of either increasing or decreasing polygenic risk scores.

This study has a limitation. Our gene-gene interaction analysis did not include other clinical covariates such as body weight or body mass index, blood pressure, lipids, hypertension, diabetes mellitus, and other risk factors because inclusion of additional clinical covariates will exclude too many subjects without such data, which will significantly reduce the discovering power of gene-gene interaction analysis. It is also likely that adjusting for covariates may reduce the significance of the current results.

In summary, the data in this study demonstrate the effectiveness of an interesting strategy to detect epistasis involved in phenotypic determination of human diseases. Our data further support the hypothesis that

ANRIL is the causal gene for CAD at the 9p21.3 locus, and *TMEM106B* is the causal gene at the 7q21.11 CAD locus. Mechanistically, *TMEM106B* regulates endothelial functions and atherosclerosis in connection with long non-coding RNA *ANRIL*. Knockdown of *TMEM106B* fully rescued *ANRIL* knockdown phenotypes in endothelial cells involved in atherosclerosis, whereas overexpression of *TMEM106B* fully rescued *ANRIL* overexpression phenotypes. Moreover, *TMEM106B* is upregulated in CAD coronary arteries. Our study also identified 2 pairs of novel gene-gene interactions (epistasis) involved in CAD, a pair involving the *ANRIL* locus and the *TMEM106B* locus and the other pair involving the *ADTRP* locus and the *MIA3* locus. Identification of epistasis is paramount to our understanding of the genetic architecture of a human disease, and may have an important implication on future precision diagnosis and risk stratification of common human diseases based on polygenic risk scores and other methods.

ARTICLE INFORMATION

Received July 30, 2019; accepted February 5, 2020.

Affiliations

From the College of Life Sciences, Lanzhou University, Lanzhou, Gansu Province, P. R. China (Y.L.); Department of Cardiovascular and Metabolic Sciences, Lerner Research Institute, Cleveland Clinic, Cleveland, OH (Y.L., H.C., F.W., S.A., Q.C., Q.K.W.); Department of Molecular Medicine, Cleveland Clinic Lerner College of Medicine of Case Western Reserve University, Cleveland, OH (Y.L., H.C., F.W., S.A., Q.C., Q.K.W.); Department of Genetics and Genome Sciences, Case Western Reserve University School of Medicine, Cleveland, OH (H.C., Q.K.W.); MRC Human Genetics Unit at the MRC IGMM, Western General Hospital, University of Edinburgh, United Kingdom (O.C.-X., A.T.); The Roslin Institute, Royal (Dick) School of Veterinary Studies, The University of Edinburgh, Easter Bush Campus, Midlothian, Edinburgh, Scotland (O.C.-X., K.R., A.T.); Key Laboratory of Molecular Biophysics, College of Life Science and Technology, Huazhong University of Science and Technology, Wuhan, Hubei, China (C.L., C.X.).

Acknowledgments

We greatly appreciate earlier initiating work on *TMEM106B* by Dr. Fan. Thanks to Ms. Annabel Z. Wang. Wang at Harvard Medical School and other members of Wang laboratory for helpful discussion and assistance.

Author contributions: Study design: Q. K. Wang, Xu, Cho, Li, and Chen; Experiments on *ANRIL*, *TMEM100* and *TMEM106B*: Cho, and Li; Experiments on *MIA3* and *ADTRP* (Figure 10): Luo; Association analysis of *TMEM100* and *TMEM106B* variants: F. Wang; Gene-gene interaction analysis: Canela-Xandri, Rawlik, and Tenesa; Data analysis: all authors; Drafting manuscript: Cho, Li, F. Wang, Chen, and Q. K. Wang; Revision of manuscript: all authors; Study supervision: Q. K. Wang, Xu, and Chen.

Sources of Funding

This work was supported by National Institutes of Health/National Heart, Lung, and Blood Institute grants R01 HL121358 (Q. K. Wang), R01 HL126729 (Q. K. Wang), and R01 HL138465 (Q. K. Wang and Chen) and in part by China Natural Science Foundation grant 31430047 (Xu). This research has been conducted using the UK Biobank Resource under project 8447. Tenesa, and Rawlik acknowledge funding from the Medical Research Council grant MR/P015514/1, UK Research and Innovation Biotechnology and Biological Sciences Research Council grant BBS/E/D/30002276 and the Medical Research Council grant MR/N003179/1, and Canela-Xandri from the Medical Research Council fellowship MR/R025851/1.

Disclosures

None.

REFERENCES

1. Wang Q. Molecular genetics of coronary artery disease. *Curr Opin Cardiol.* 2005;20:182–188.
2. Wang Q. Advances in the genetic basis of coronary artery disease. *Curr Atheroscler Rep.* 2005;7:235–241.
3. Musunuru K, Kathiresan S. Genetics of common, complex coronary artery disease. *Cell.* 2019;177:132–145.
4. Lo Sardo V, Chubukov P, Ferguson W, Kumar A, Teng EL, Duran M, Zhang L, Cost G, Engler AJ, Urnov F, et al. Unveiling the role of the most impactful cardiovascular risk locus through haplotype editing. *Cell.* 2018;175:1796–1810.e20.
5. Cho H, Shen GQ, Wang X, Wang F, Archacki S, Li Y, Yu G, Chakrabarti S, Chen Q, Wang QK. Long noncoding RNA *ANRIL* regulates endothelial cell activities associated with coronary artery disease by up-regulating *CLIP1*, *EZR*, and *LYVE1* genes. *J Biol Chem.* 2019;294:3881–3898.
6. Somekawa S, Imagawa K, Hayashi H, Sakabe M, Ioka T, Sato GE, Inada K, Iwamoto T, Mori T, Uemura S, et al. *Tmem100*, an ALK1 receptor signaling-dependent gene essential for arterial endothelium differentiation and vascular morphogenesis. *Proc Natl Acad Sci USA.* 2012;109:12064–12069.
7. Mizuta K, Sakabe M, Hashimoto A, Ioka T, Sakai C, Okumura K, Hattamaru M, Fujita M, Araki M, Somekawa S, et al. Impairment of endothelial-mesenchymal transformation during atrioventricular cushion formation in *Tmem100* null embryos. *Dev Dyn.* 2015;244:31–42.
8. Moon EH, Kim YS, Seo J, Lee S, Lee YJ, Oh SP. Essential role for *TMEM100* in vascular integrity but limited contributions to the pathogenesis of hereditary haemorrhagic telangiectasia. *Cardiovasc Res.* 2015;105:353–360.
9. Kundu ST, Grzeskowiak CL, Fradette JJ, Gibson LA, Rodriguez LB, Creighton CJ, Scott KL, Gibbons DL. *TMEM106B* drives lung cancer metastasis by inducing TFEB-dependent lysosome synthesis and secretion of cathepsins. *Nat Commun.* 2018;9:2731.
10. Stagi M, Klein ZA, Gould TJ, Bewersdorf J, Strittmatter SM. Lysosome size, motility and stress response regulated by fronto-temporal dementia modifier *TMEM106B*. *Mol Cell Neurosci.* 2014;61:226–240.
11. Brady OA, Zheng Y, Murphy K, Huang M, Hu F. The frontotemporal lobar degeneration risk factor, *TMEM106B*, regulates lysosomal morphology and function. *Hum Mol Genet.* 2013;22:685–695.
12. Wang F, Xu CQ, He Q, Cai JP, Li XC, Wang D, Xiong X, Liao YH, Zeng QT, Yang YZ, et al. Genome-wide association identifies a susceptibility locus for coronary artery disease in the Chinese Han population. *Nat Genet.* 2011;43:345–349.
13. Tayebi N, Ke T, Foo JN, Friedlander Y, Liu J, Heng CK. Association of single nucleotide polymorphism rs6903956 on chromosome 6p24.1 with coronary artery disease and lipid levels in different ethnic groups of the Singaporean population. *Clin Biochem.* 2013;46:755–759.
14. Li X, Huang Y, Yin D, Wang D, Xu C, Wang F, Yang Q, Wang X, Li S, Chen S, et al. Meta-analysis identifies robust association between SNP rs17465637 in *MIA3* on chromosome 1q41 and coronary artery disease. *Atherosclerosis.* 2013;231:136–140.
15. Wang AZ, Li L, Zhang B, Shen GQ, Wang QK. Association of SNP rs17465637 on chromosome 1q41 and rs599839 on 1p13.3 with myocardial infarction in an American caucasian population. *Ann Hum Genet.* 2011;38:149–156.
16. Lu Q, Yao Y, Hu Z, Hu C, Song Q, Ye J, Xu C, Wang AZ, Chen Q, Wang QK. Angiogenic factor *AGGF1* activates autophagy with an essential role in therapeutic angiogenesis for heart disease. *PLoS Biol.* 2016;14:e1002529.
17. Yao Y, Lu Q, Hu Z, Yu Y, Chen Q, Wang QK. A non-canonical pathway regulates ER stress signaling and blocks ER stress-induced apoptosis and heart failure. *Nat Commun.* 2017;8:133.
18. Archacki SR, Angheloiu G, Tian XL, Tan FL, DiPaola N, Shen GQ, Moravec C, Ellis S, Topol EJ, Wang Q. Identification of new genes differentially expressed in coronary artery disease by expression profiling. *Physiol Genomics.* 2003;15:65–74.
19. Archacki SR, Angheloiu G, Moravec CS, Liu H, Topol EJ, Wang QK. Comparative gene expression analysis between coronary arteries and internal mammary arteries identifies a role for the *TES* gene in endothelial cell functions relevant to coronary artery disease. *Hum Mol Genet.* 2012;21:1364–1373.
20. Tu X, Nie S, Liao Y, Zhang H, Fan Q, Xu C, Bai Y, Wang F, Ren X, Tang T, et al. The IL-33-ST2L pathway is associated with coronary artery disease in a Chinese Han population. *Am J Hum Genet.* 2013;93:652–660.

21. You SA, Archacki SR, Angheloiu G, Moravec CS, Rao S, Kinter M, Topol EJ, Wang Q. Proteomic approach to coronary atherosclerosis shows ferritin light chain as a significant marker: evidence consistent with iron hypothesis in atherosclerosis. *Physiol Genomics*. 2003;13:25–30.
22. Bai Y, Nie S, Jiang G, Zhou Y, Zhou M, Zhao Y, Li S, Wang F, Lv Q, Huang Y, et al. Regulation of CARD8 expression by ANRIL and association of CARD8 single nucleotide polymorphism rs2043211 (p.C10X) with ischemic stroke. *Stroke*. 2014;45:383–388.
23. Chen S, Wang X, Wang J, Zhao Y, Wang D, Tan C, Fa J, Zhang R, Wang F, Xu C, et al. Genomic variant in CAV1 increases susceptibility to coronary artery disease and myocardial infarction. *Atherosclerosis*. 2016;246:148–156.
24. Luo C, Pook E, Tang B, Zhang W, Li S, Leineweber K, Cheung SH, Chen Q, Bechem M, Hu JS, et al. Androgen inhibits key atherosclerotic processes by directly activating ADTRP transcription. *Biochim Biophys Acta Mol Basis Dis*. 2017;1863:2319–2332.
25. Luo C, Wang F, Qin S, Chen Q, Wang Q. Coronary artery disease susceptibility gene ADTRP regulates cell cycle progression, proliferation and apoptosis by global gene expression regulation. *Physiol Genomics*. 2016;48:554–564.
26. Luo CY, Wang F, Ren X, Ke T, Xu CQ, Tang B, Qin SB, Yao YF, Chen QY, Wang QK. Identification of a molecular signaling gene-gene regulatory network between GWAS susceptibility genes ADTRP and MIA3/TANGO1 for coronary artery disease. *Biochim Biophys Acta Mol Basis Dis*. 2017;1863:1640–1653.
27. Wang J, Fa J, Wang P, Jia X, Peng H, Chen J, Wang Y, Wang C, Chen Q, Tu X, et al. NINJ2- a novel regulator of endothelial inflammation and activation. *Cell Signal*. 2017;35:231–241.
28. Nikpay M, Goel A, Won HH, Hall LM, Willenborg C, Kanoni S, Saleheen D, Kyriakou T, Nelson CP, Hopewell JC, et al. A comprehensive 1,000 Genomes-based genome-wide association meta-analysis of coronary artery disease. *Nat Genet*. 2015;47:1121–1130.
29. Canela-Xandri O, Rawlik K, Tenesa A. An atlas of genetic associations in UK Biobank. *Nat Genet*. 2018;50:1593–1599.
30. Magi R, Morris AP. GWAMA: software for genome-wide association meta-analysis. *BMC Bioinformatics*. 2010;11:288.
31. Wang L, Wang X, Wang L, Yousaf M, Li J, Zuo M, Yang Z, Gou D, Bao B, Li L, et al. Identification of a new adtrp1-tfpi regulatory axis for the specification of primitive myelopoiesis and definitive hematopoiesis. *FASEB J*. 2018;32:183–194.
32. Patel MM, Behar AR, Silasi R, Regmi G, Sansam CL, Keshari RS, Lupu F, Lupu C. Role of ADTRP (androgen-dependent tissue factor pathway inhibitor regulating protein) in vascular development and function. *J Am Heart Assoc*. 2018;7:e010690. DOI: 10.1161/JAHA.118.010690.
33. Raote I, Ortega-Bellido M, Santos AJ, Foresti O, Zhang C, Garcia-Parajo MF, Campelo F, Malhotra V. TANGO1 builds a machine for collagen export by recruiting and spatially organizing COPII, tethers and membranes. *Elife*. 2018;7:e32723.
34. Klein ZA, Takahashi H, Ma M, Stagi M, Zhou M, Lam TT, Strittmatter SM. Loss of TMEM106B ameliorates lysosomal and frontotemporal dementia-related phenotypes in progranulin-deficient mice. *Neuron*. 2017;95:281–296.e6.
35. Hendriks T, Walenbergh SM, Hofker MH, Shiri-Sverdlov R. Lysosomal cholesterol accumulation: driver on the road to inflammation during atherosclerosis and non-alcoholic steatohepatitis. *Obes Rev*. 2014;15:424–433.
36. Xu X, Yuan X, Li N, Dewey WL, Li PL, Zhang F. Lysosomal cholesterol accumulation in macrophages leading to coronary atherosclerosis in CD38(-/-) mice. *J Cell Mol Med*. 2016;20:1001–1013.
37. Emanuel R, Sergin I, Bhattacharya S, Turner J, Epelman S, Settembre C, Diwan A, Ballabio A, Razani B. Induction of lysosomal biogenesis in atherosclerotic macrophages can rescue lipid-induced lysosomal dysfunction and downstream sequelae. *Arterioscler Thromb Vasc Biol*. 2014;34:1942–1952.
38. Sergin I, Evans TD, Zhang X, Bhattacharya S, Stokes CJ, Song E, Ali S, Dehestani B, Holloway KB, Micevych PS, et al. Exploiting macrophage autophagy-lysosomal biogenesis as a therapy for atherosclerosis. *Nat Commun*. 2017;8:15750.
39. Zhang EB, Kong R, Yin DD, You LH, Sun M, Han L, Xu TP, Xia R, Yang JS, De W, et al. Long noncoding RNA ANRIL indicates a poor prognosis of gastric cancer and promotes tumor growth by epigenetically silencing of miR-99a/miR-449a. *Oncotarget*. 2014;5:2276–2292.
40. Sarkar D, Leung EY, Baguley BC, Finlay GJ, Askarian-Amiri ME. Epigenetic regulation in human melanoma: past and future. *Epigenetics*. 2015;10:103–121.
41. Meseure D, Vacher S, Alsibai KD, Nicolas A, Chemlali W, Caly M, Lidereau R, Pasmant E, Callens C, Bieche I. Expression of ANRIL-polycomb complexes-CDKN2A/B/ARF genes in breast tumors: identification of a two-gene (EZH2/CBX7) signature with independent prognostic value. *Mol Cancer Res*. 2016;14:623–633.
42. Chi JS, Li JZ, Jia JJ, Zhang T, Liu XM, Yi L. Long non-coding RNA ANRIL in gene regulation and its duality in atherosclerosis. *J Huazhong Univ Sci Technolog Med Sci*. 2017;37:816–822.
43. Wang Y, Cheng N, Luo J. Downregulation of lncRNA ANRIL represses tumorigenicity and enhances cisplatin-induced cytotoxicity via regulating microRNA let-7a in nasopharyngeal carcinoma. *J Biochem Mol Toxicol*. 2017;31:e21904. Available at: <https://doi.org/10.1002/jbt.21904>.
44. Deng W, Chen K, Liu S, Wang Y. Silencing circular ANRIL protects HK-2 cells from lipopolysaccharide-induced inflammatory injury through up-regulating microRNA-9. *Artif Cells Nanomed Biotechnol*. 2019;47:3478–3484.
45. Shu L, Zhang W, Huang C, Huang G, Su G, Xu J. LncRNA ANRIL protects H9c2 cells against hypoxia-induced injury through targeting the miR-7-5p/SIRT1 axis. *J Cell Physiol*. 2020;235:1175–1183.
46. Liu B, Cao W, Xue J. LncRNA ANRIL protects against oxygen and glucose deprivation (OGD)-induced injury in PC-12 cells: potential role in ischaemic stroke. *Artif Cells Nanomed Biotechnol*. 2019;47:1384–1395.
47. Guo F, Tang C, Li Y, Liu Y, Lv P, Wang W, Mu Y. The interplay of LncRNA ANRIL and miR-181b on the inflammation-relevant coronary artery disease through mediating NF-kappaB signalling pathway. *J Cell Mol Med*. 2018;22:5062–5075.
48. Tan P, Guo YH, Zhan JK, Long LM, Xu ML, Ye L, Ma XY, Cui XJ, Wang HQ. LncRNA-ANRIL inhibits cell senescence of vascular smooth muscle cells by regulating miR-181a/Sirt1. *Biochem Cell Biol*. 2019;97:571–580.
49. He ZY, Wei TH, Zhang PH, Zhou J, Huang XY. Long noncoding RNA-antisense noncoding RNA in the INK4 locus accelerates wound healing in diabetes by promoting lymphangiogenesis via regulating miR-181a/Prox1 axis. *J Cell Physiol*. 2019;234:4627–4640.
50. Phillips PC. Epistasis—the essential role of gene interactions in the structure and evolution of genetic systems. *Nat Rev Genet*. 2008;9:855–867.
51. Nghe P, Kogenaru M, Tans SJ. Sign epistasis caused by hierarchy within signalling cascades. *Nat Commun*. 2018;9:1451.